

Article

Formulation and Characterization of a Novel Palm-Oil-Based α -Mangostin Nano-Emulsion (PO-AMNE) as an Antimicrobial Endodontic Irrigant: An In Vitro Study

Omer Sheriff Sultan ^{1,*}, Haresh Kumar A/L Kantilal ², Khoo Suan Phaik ¹, Hira Choudhury ³ and Fabian Davamani ^{4,*} 

¹ School of Dentistry, International Medical University, Kuala Lumpur 57000, Malaysia

² School of Medicine, International Medical University, Kuala Lumpur 57000, Malaysia

³ School of Pharmacy, International Medical University, Kuala Lumpur 57000, Malaysia

⁴ School of Health Sciences, International Medical University, Kuala Lumpur 57000, Malaysia

* Correspondence: omersheriff@imu.edu.my (O.S.S.); fabian_davamani@imu.edu.my (F.D.); Tel.: +60-173987864 (O.S.S.)

Abstract: Aim: To formulate and characterize a palm-oil-in-water-based α -Mangostin nano-emulsion (PO-AMNE) endodontic irrigant, in order to evaluate its antibacterial efficacy against *Enterococcus faecalis*, *Staphylococcus epidermidis*, and *Candida albicans* biofilms, as well as its capacity to remove smear layer. Methods: The solubility of α -Mangostin in various oils was determined and selected, surfactants and co-surfactants were used for the nano-emulsion trial. PO-AMNE was prepared and optimized. The MIC was performed, and the antimicrobial efficacy was estimated against biofilms. The optimized 0.2% PO-AMNE irrigant antimicrobial efficacy in a tooth model was done using colony-forming units. The treated teeth were processed by scanning electron microscopic examination for debris and smear layer removal. An Alamar Blue assay was used to evaluate cell viability. The optimization of the PO-AMNE irrigant was performed using Box–Behnken statistical design. Results: The optimized 0.2% PO-AMNE irrigant was found to have a particle size of 340.9 nm with 0.246 PDI of the dispersed droplets, and a zeta potential (mV) of -27.2 ± 0.7 mV. The MIC values showed that 0.2% PO-AMNE (1.22 ± 0.02) were comparable to 2% CHX (1.33 ± 0.01), and 3.25% NaOCl (2.2 ± 0.09) had the least inhibition for *E. faecalis*. NaOCl (3.25%) showed the maximum inhibition of *S. epidermidis* (0.26 ± 0.05), whereas 0.2% PO-AMNE (1.25 ± 0.0) was comparable to 2% CHX (1.86 ± 0.07). For *C. albicans*, 2% CHX (8.12 ± 0.12) showed the least inhibition as compared to 0.2% PO-AMNE (1.23 ± 0.02) and 3.25% NaOCl (0.59 ± 0.02). The 0.2% PO-AMNE irrigant was then evaluated for its antimicrobial efficacy against the three biofilms, using colony-forming units. The 0.2% PO-AMNE was comparable to both 3.25% NaOCl and 2% CHX in inhibiting the growth of biofilms. The 0.2% PO-AMNE and 17% EDTA eliminated the smear layer with the lowest mean scores ($p < 0.001$). Finally, 0.2% PO-AMNE was shown to be biocompatible when compared to 17% EDTA, 3.25% NaOCl, and 2% CHX in immortalized oral keratinocyte cells. Conclusion: Overall, the formulated 0.2% PO-AMNE irrigant was an effective antimicrobial and biocompatible which could combat endodontic-infection-related polymicrobial biofilms.

Keywords: palm oil; α -Mangostin; nano-emulsion; antimicrobial; endodontic irrigant



Citation: Sultan, O.S.; Kantilal, H.K.A./L.; Phaik, K.S.; Choudhury, H.; Davamani, F. Formulation and Characterization of a Novel Palm-Oil-Based α -Mangostin Nano-Emulsion (PO-AMNE) as an Antimicrobial Endodontic Irrigant: An In Vitro Study. *Processes* **2023**, *11*, 798. <https://doi.org/10.3390/pr11030798>

Academic Editors: Ibrahim M. Abu-Reidah and Paolo Trucillo

Received: 2 February 2023
Revised: 10 February 2023
Accepted: 26 February 2023
Published: 7 March 2023



Copyright: © 2023 by the authors. Licensee MDPI, Basel, Switzerland. This article is an open access article distributed under the terms and conditions of the Creative Commons Attribution (CC BY) license (<https://creativecommons.org/licenses/by/4.0/>).

1. Introduction

Medicinal plants are an inexhaustible source of novel bioactive compounds which have a promising future in medicine [1,2]. Mangosteen (*Garcinia mangostana* Linn) is a fruit that grows in Asian countries, such as Malaysia, Myanmar, Thailand, the Philippines, Sri Lanka, and India. α -Mangostin, a natural xanthone produced from the pericarp of mangosteen, has been documented for its distinct pharmacological activities [3]. This compound has been shown to possess antibacterial [4], antifungal [5], and antiparasitic

properties [6]. Multi-species biofilms cause infections of the root canal system in teeth and periradicular tissues, and microbial persistence appears to have a major role in the endodontic treatment outcome [7]. In cases of failed endodontic therapy and canals with persistent infections, *Enterococcus faecalis* (*E. faecalis*) and yeast, primarily *Candida albicans* (*C. albicans*), have been repeatedly identified. [8,9]. Murad et al. (2014) reported that *Staphylococcus epidermidis* (*S. epidermidis*) plays an important role in persistent endodontic infections [10]. Various studies have evaluated the effects of α -Mangostin on *E. faecalis*, *S. epidermidis*, and *C. albicans*. Flavonoids derived from the mangosteen pericarp were found to be effective against *E. faecalis* bacterial biofilm [11].

The instrumentation during the shaping of canals leads to organic and inorganic remnants on the canal, leading to an uneven and granular layer called the smear layer [12]. This layer obstructs the dentinal tubules by reducing dentinal permeability, delaying the action of topical medications and irrigants, and preventing close contact of the filling material with the dentinal walls [13]. As a result, there is an increased risk of bacterial infection and failure [14]. Removing the smear layer leads to better irrigant interaction with canal walls, resulting in improved cleaning and closer interfacial proximity between root canal fillings and dentin. Citric acid has been commonly employed to remove the smear layer, which has strong chemical stability, is inexpensive [15], and has excellent results [16,17].

Root canal irrigants have been used as an adjunct to enhance the antibacterial effect of cleaning and shaping in endodontic treatment for many years. Because of its dissolving action on pulp tissue and antibacterial activity, sodium hypochlorite (NaOCl) is the most commonly used irrigant in the treatment of infected root canals. However, when injected into periapical tissues, it has a cytotoxic effect, leaves a bad odor and taste, has a corrosive potential, and may cause allergic reactions [18]. Chlorhexidine (CHX) is a cationic bisbiguanide and has been used as an irrigating solution during root canal treatment due to its broad antibacterial activity. However, the use of CHX as a root canal irrigant is limited because it has no tissue solvent activity and some patients may have allergic reactions to it [19]; additionally, it can discolor teeth [20]. Previous research has shown that both NaOCl and CHX were highly cytotoxic to human periodontal ligament (PDL) cells, by inhibiting mitochondrial activity [21]. As a result, there is a growing need for irrigants with effective antimicrobial properties that are also biocompatible with oral tissues.

Nano-emulsions are colloidal systems that are made up of two immiscible phases, and are translucent, with droplet sizes ranging from 50 to 500 nm. Surfactants, or a mixture of surfactants and co-surfactants, are used to kinetically stabilize these systems and reduce the droplet size of the nano-emulsion [22,23]. Controlling medication release and providing a wide range of therapeutic agents are two main advantages of nano-emulsions [24]. Furthermore, they outperform macroemulsions in terms of surface area and free energy, and coalescence, flocculation, creaming, and sedimentation are also avoided. Nano-emulsions can be made with lower emulsifying agent concentrations, lowering surfactant-related toxicity [25].

The antimicrobial efficacy of α -Mangostin nano-emulsion was evaluated against *E. faecalis*, *S. epidermidis*, and *C. albicans* biofilms, as these species cause the most prevalent root canal infections. *E. faecalis* is a microorganism that is detected in persistent and asymptomatic endodontic infections, which is quite prevalent in such infections ranging from 24% to 77% [26]. Palm oil is a medium-chain fatty-acid-rich source of lauric acid (LA). Hess et al., 2015 [27] and Hinton and Ingram (2006) [28] found that LA inhibited the formation of *E. faecalis* biofilms, while Krishnapriya et al. (2019) reported that LA was effective against *C. albicans* [29]. *S. epidermidis* is also a Gram-positive facultative anaerobic bacterium that infects the root canal and stays in a benign relationship with the host. Moreover, this is an opportunistic pathogen, as it invades the host defenses like antimicrobial peptides (AMPs) on human skin and penetrates the epithelial barrier [30].

Our work aims to formulate and characterize an α -Mangostin oil-in-water nano-emulsion-based endodontic irrigant, targeting antimicrobial efficacy against *E. faecalis*, *S. epidermidis*, and *C. albicans* biofilms with smear layer removal capability. In addition, it will be tested for biocompatibility in immortalized oral keratinocyte OKF-6 cells.

2. Materials and Methods

The α -Mangostin (purity > 95%) was procured from Chengdu Biopurify Phytochemicals (China). The procurement of palm oil, olive oil, and avocado was done from Country Farms Sdn Bhd (Malaysia). The macadamia oil was procured from Macadamia Nut Oil, Malaysia, almond oil from IN-SCENT (USA), and primrose oil from iHerb (Malaysia). The surfactants Tween 80, Tween 20, glycerol, and Span 80 were obtained from Merck, Sigma-Aldrich, St. Louis, USA. The other surfactants, Lipophile, Labrafac™ PG, Labrafil CS, and Peceol, were gifted by Gattefosse, Saint Priest, France. The Maisine and Transcutol HP co-surfactants were procured from Gattefosse, Saint Priest, France. The dialysis membrane (12 kDa cut-off) was purchased from HiMedia Laboratories Mumbai, India. A low-speed diamond saw was obtained from Buehler (Isomet, Buehler Ltd., Lake Bluff, IL, USA). A Gates Glidden drill was obtained from Mani®, Utsunomiya, Tochigi, Japan and the low-speed handpiece was obtained from Kavo, Charlotte, NC, USA). The K-files and ProTaper Universal rotary system were obtained from Dentsply, Maillefer, Ballaigues, Switzerland.

2.1. Development of PO-AMNE: Formulation and Characterization

Various oils, surfactants, and co-surfactants were employed to evaluate the solubility of α -Mangostin during the selection of components for the development of PO-AMNE.

2.1.1. Selection of Suitable Internal Phase (Oil): Screening of Oils for α -Mangostin Nano-Emulsion Development

α -Mangostin was added to the oils every 6–12 h, until the additive was no longer visibly soluble. To establish equilibrium, the mixture was maintained for 72 h at 37 °C in a shaking water bath incubator, at 100 rpm. α -Mangostin was added every 24 h, until it could no longer be visually dissolved. After 72 h, the samples were centrifuged for 15 min to produce the residue, which was diluted with methanol (Solution A) and filtered through a 0.22 mm membrane filter [31]. α -Mangostin concentration was determined using the UV spectrophotometric technique, at a wavelength of 248 nm.

2.1.2. Selection of Surfactants and Co-Surfactants

α -Mangostin was added to the surfactants and co-surfactants every 6–12 h, until the additive was no longer visibly soluble. The absorbance of the diluted sample was then measured at 248 nm. Then, to determine the final surfactant and co-surfactant, 1 mL of each, with a combination of palm oil, was added dropwise, followed by 1 min of vortexing. This was performed until the mixture turned turbid. Each sample was performed in triplicate. For the nano-emulsion test, the chosen surfactant and co-surfactant were used [31].

2.1.3. Preparation of PO-AMNE

The PO-AMNE was prepared by high-pressure homogenization for 3 cycles, alongside an aqueous titration method, based on the different ratios of the components as suggested by the software. The weighed quantity of the drug was added to the oil and stirred until complete solubilization was achieved. The mixtures of surfactants, acid, and water were added into the respective tubes in specific ratios, followed by the dropwise addition of an aqueous phase with continuous vortex-mixing, to form a clear, transparent, and homogeneous PO-AMNE. Finally, the clear, transparent, or slightly whitish PO-AMNEs were evaluated for the droplet size, polydispersity index (PDI), and zeta potential, using Zetasizer (Nano-ZS90, Malvern Instruments, Worcestershire, UK).

2.2. Thermodynamic Stability Testing of α -Mangostin Nano-Emulsion

2.2.1. Centrifugation Test

All formulations were centrifuged at 5000 rpm for 30 min and checked for phase separation, creaming, and/or cracking. The homogenous stable formulations were chosen for further research after triple testing [31].

2.2.2. Heating–Cooling Cycle

To determine the temperature effect formulation stability, formulations were kept at 40 °C and 4 °C for 48 h, in three cycles. After this, formulations were observed for any instability (phase separation, turbidity, etc.) [31].

2.2.3. Freeze–Thaw Cycle

Three freeze–thaw cycles at –20 °C and 25 °C, for 48 h each, were used to assess thermodynamically stable materials. Creaming, cracking, and phase separation was examined after the freeze–thaw cycles. To identify any drastic change in the droplet size, PDI, and surface charge, these parameters of all the stable formulations were compared [31].

2.3. Box–Behnken Statistical Design: Optimization of the α -Mangostin Nano-Emulsion (PO-AMNE)

According to the literature, oil and surfactant percentages play a significant influence in achieving the ideal droplet size and polydispersity index in nano-emulsion formulation [31,32]. In addition, the cosolvent may have affected the physical properties of nano-emulsions [33]. Therefore, in this optimization process, the percentage of oil (palm oil), percentage of Smix (Span 80: Tween 80::1:2), and percentage of cosolvent in nano-emulsion formulation were regarded as independent variables, and their effects on droplet size and polydispersity index of the nano-emulsion were investigated using a three-factor, three-level Box–Behnken statistical design (Design Expert[®], version 12; State-Ease Inc., Minneapolis, MN, USA).

Three levels of the three independent variables were determined and included in the software [33] based on our preliminary studies and literature data. The droplet size and polydispersity index of each formulation were analyzed based on the software's recommendation of 17 batches, containing a combination of different levels of independent variables (Table 1). In addition, based on the experimental data of the droplet size and the PDI of the suggested 17 formulations, the software was used to obtain the software-recommended optimal formulation. Analysis of variance (ANOVA) was used to analyze the interaction of three independent variables with their three-level dependent variables.

In addition, the effect of the interaction of the three independent variables on droplet size and PDI was illustrated using software-generated perturbation plots, experimental versus predicted plot contour plots, and 3D surface plots.

$$Y = b_0 + b_1A + b_2B + b_3C + b_{12}AB + b_{13}AC + b_{23}BC + b_{11}A^2 + b_{22}B^2 + b_{33}C^2 \quad (1)$$

where Y represents dependent variables, droplet size, and PDI, whereas b_0 is the intercept, and the coefficient for the respective model, where the terms are represented by b_1 , b_2 , b_3 , b_{12} , b_{13} , b_{23} , b_{11} , b_{22} , and b_{33} [34].

2.3.1. Measurement of Droplet Size, Polydispersity Index, and Zeta Potential

Using Zetasizer, the mean droplet size and degree of droplet size distribution were analyzed. Using the same instrument, the surface charge of the formulations was measured. As stated previously, thermodynamic stability studies were conducted on the developed PO-AMNE.

Table 1. Box–Behnken Design: three independent variables and their three levels.

| Batch | Level of Independent Variables | | |
|---|--------------------------------|------------|----------|
| | A | B | C |
| F1 | −1 | 0 | −1 |
| F2 | 1 | 0 | 1 |
| F3 | 0 | 0 | 0 |
| F4 | 1 | 0 | −1 |
| F5 | 0 | 0 | 0 |
| F6 | 0 | 1 | −1 |
| F7 | 0 | 0 | 0 |
| F8 | −1 | 1 | 0 |
| F9 | 1 | 1 | 0 |
| F10 | −1 | −1 | 0 |
| F11 | 0 | −1 | 1 |
| F12 | 0 | 0 | 0 |
| F13 | 1 | −1 | 0 |
| F14 | 0 | 0 | 0 |
| F15 | −1 | 0 | 1 |
| F16 | 0 | 1 | 1 |
| F17 | 0 | −1 | −1 |
| Independent variable | Levels | | |
| | Low (−1) | Medium (0) | High (1) |
| A = Oil (% v/v) | 5 | 7.5 | 10 |
| B = Smix (% v/v) Smix :: Span 80: tween 80 :: 1:2 | 9 | 15 | 21 |
| C = Glycerol (% v/v) | 10 | 15 | 20 |
| Dependent variables | | | |
| Y1 = Droplet size (nm) | | | |

2.3.2. Preparation of Optimized Palm-Oil-Based α -Mangostin Nano-Emulsion (PO-AMNE)

α -Mangostin-loaded oil-in-water nano-emulsions (NEs) were formulated with the same proportions of palm oil, Smix, 10% citric acid, and aqueous phases as the optimized formulation. The low energy emulsification technique was utilized to formulate the drug-loaded NE formulation, in which 20 mg α -Mangostin was dissolved in the oil phase, followed by the addition of Smix, acid, and aqueous phase to yield 10 mL of the NE formulation (0.2% PO-AMNE).

2.3.3. Transmission Electron Microscopy (TEM)

Transmission electron microscopic evaluation was performed to determine the structure and morphology of the formulated PO-AMNE. A drop of the 100-fold diluted sample was placed on a 300-mesh carbon-coated copper grid for analysis. Finally, 2% phosphotungstic acid was used to negatively stain the droplets, which were then examined using a 100 kV microscope [35].

2.4. Antimicrobial Studies

2.4.1. Microorganisms

E. faecalis, *S. epidermidis*, and *C. albicans* in the biofilms formed in the microtiter dish were quantified directly by counting the microbial cells adhering to the surface. For the identification of any metabolic alterations of three test organisms, *E. faecalis*, *S. epidermidis*, and *C. albicans*, an analytical profile index (API) identification scheme had been used [36,37].

2.4.2. Determination of Minimum Inhibitory Concentration (MIC)

For the present study, MIC was performed for *E. faecalis*, *S. epidermidis*, and *C. albicans*. The concentration of α -Mangostin nano-emulsion that has been used for the study is 0.2% of α -Mangostin [38].

2.4.3. Micro Dilution Method

Here, the MIC of PO-AMNE against *E. faecalis*, *S. epidermidis*, and *C. albicans* chloride (TTC) was used as an indicator [39].

2.4.4. Biofilm Assay (Microtiter Plate)

Bacteria are incubated at the “U”-shaped bottom of 96-well microtiter plates, in order to observe the adherence of bacteria to an abiotic surface. Cells that are adhered to the wells get stained for visualization [40].

2.5. Ex Vivo Experiment—Antimicrobial Efficacy—0.2% PO-AMNE Irrigant in a Tooth Model Using Colony-Forming Units (CFU)

2.5.1. Tooth Sample Preparation

One hundred sixty freshly extracted caries-free single-rooted mandibular premolars extracted for orthodontic treatment were collected from patients with their informed consent in accordance with a protocol, reviewed and approved by the Institutional Review Board of International Medical University, Joint Committee on Research and Ethics for the research project ID: PMHS I-2018 (01). In this research, the experiment model was a modified version of the Haapasalo and Orstavik tooth model that included bovine teeth. This model was used because it offered a more accurate simulation of clinical circumstances for evaluating the antimicrobial efficacy of endodontic irrigants in dentinal tubules. To evaluate the CFU, one hundred and sixty dentin blocks were prepared. These teeth specimens of 8 mm width were obtained by removing the crowns (2–3 mm from the cement–enamel junction), and 3 to 5 mm of the apical portion of the root, using a low-speed diamond saw (Isomet, Buehler Ltd., Lake Bluff, IL, USA). The inner diameter of the root canals of each sample was standardized using a Gates Glidden size 3 (Mani[®], Utsunoniya, Tochigi, Japan) drill at 300 rpm with a low-speed handpiece (Kavo, Charlotte, NC, USA) [41].

2.5.2. Antimicrobial Assessment Using Colony-Forming Units (CFU)

The CFU measurement technique was used to estimate the antimicrobial efficacy of a nano-formulation irrigant in tooth models. The *E. faecalis*, *S. epidermidis*, and *C. albicans* were grown overnight in a BHI broth [42]. Each dentin block was submerged in microcentrifuge tubes containing BHIA (Brain Heart Infusion Agar) broth that had been pre-sterilized. To contaminate the dentin block, 50 μ L of the overnight culture of *E. faecalis*, *S. epidermidis*, and *C. albicans* cultures were placed in each microcentrifuge tube. On BHIA (Brain Heart Infusion Agar) plates, 5 μ L of the broth from the incubated dentin blocks was subcultured to determine the purity of the culture. The samples of teeth were irrigated. The dentin blocks were randomly divided into four groups of 10 specimens for each organism (*E. faecalis*, *S. epidermidis*, and *C. albicans*): group 1: 0.2% PO-AMNE, group 2: 2% CHX (CHX), group 3: 3.25% NaOCl, and group 4: saline (control). After irrigation, bacterial growth was evaluated by harvesting dentin chips at 200 μ m and 400 μ m with Gates Glidden drills No. 4 and No. 5 (Mani[®], Utsunoniya, Tochigi, Japan), respectively [43].

2.6. Smear Layer Removal in Tooth Model

To perform this experiment, 30 extracted human single-rooted premolars were selected for this study. The samples were randomly divided into 3 groups ($n = 10$), where treatments were as follows: group 1: 0.2% PO-AMNE, group 2: 17% EDTA and group 3: saline.

Access cavities were prepared and working lengths were determined by deducting 1 mm from the length at which the file was barely visible to the naked eye at the apical foramen. Using the ProTaper Universal rotary system (Dentsply, Maillefer, Ballaigues, Switzerland), canals were prepared. Each canal was finished with a #F3 apical preparation. Each solution (30 mL) was used to determine the effects of experimental and control solutions as a final rinse on the surface of root canals after instrumentation, for a total duration of one minute. A 30-gauge side-vented needle (Dentsply Tulsa Dental, Tulsa, OK, USA) was passively placed within the middle third of the root canals to deliver the irrigating solution. The teeth were then divided longitudinally into two halves. The samples were then scheduled for scanning electron microscopic (SEM) evaluation [44].

2.6.1. Selection of Representative SEM Sections

After the central beam of the SEM had been directed to the center of the object by the SEM operator at $10\times$ magnification, the magnification was increased to $200\times$ and subsequently, $1000\times$, respectively, and the canal wall region appearing on the screen was photographed [45].

2.6.2. SEM Analysis and Scoring

The smear layer score systems, introduced by Hülsmann et al., [45] were followed to score the smear layer (Table 2). These scoring systems were applied to the coronal, middle, and apical thirds of the canal [45].

Table 2. Scoring criteria for smear layer evaluation.

| Score | Criteria |
|-------|---|
| 1 | Clean root canal wall and only a few small debris particles |
| 2 | A few small agglomerations of debris |
| 3 | Many agglomerations of debris covering less than 50% of the root canal wall |
| 4 | More than 50% of the root canal walls were covered with debris |
| 5 | Complete or nearly complete root canal wall coverage with debris |

The results were then dichotomized into “clean canal wall”, which included scores 1 and 2, and “smear layer present”, which included scores 3, 4, and 5.

2.7. Biocompatibility Test Using an Alamar Blue Assay on Immortalized Oral Keratinocyte OKF-6 Cells

The Alamar Blue assay was used to determine the viability of immortalized oral keratinocyte OKF-6 cells. The cells were cultured in keratinocyte serum-free medium (SFM, Thermo Fischer, Waltham, MA, USA) and seeded at a density of 1.8×10^4 cells per well in a 96-well black plate. The cells were allowed to attach overnight. The cells were then treated with group 1: 20 mgs/mL α -Mangostin, group 2: 0.2% PO-AMNE, group 3: 3.25% NaOCl, group 4: 2% CHX, and group 5: 17% EDTA. The cells were then treated for 1 min, 5 min, 10 min, 30 min, and 1 h. Later, the medium in each well was changed to a standard culture medium. Then, 10 μ L of Alamar Blue (Invitrogen, Carlsbad, CA, USA) was added to each well, followed by a 4 h incubation at 37°C and 5% carbon dioxide. Furthermore, the fluorescence of each well was measured using the FLx800 fluorescence microplate reader at 570 nm excitation and 590 nm emission wavelengths (Bio-Tek, Winooski, VT, USA) [46,47].

2.8. Statistical Analysis

The data obtained were entered manually in Microsoft Excel Data, and the data were cleaned. IBM SPSS Statistics for Windows software, Version 29.0. (IBM Corp: Armonk, NY, USA) was used for data analysis, to represent the data graphically and provide statistical analysis. The mean and standard deviation was analyzed using descriptive statistics. The normality of the data was assessed by using the Kolmogorov–Smirnov test. A one-way analysis of variance (ANOVA), with a Dunnett’s test, was used to investigate significant differences between the four groups of data that followed (differences between the four groups). To do the pair-wise comparison, a Tukey’s post-hoc test was used. The significance level was set at $p < 0.05$.

3. Results

3.1. Formulation and Characterization of PO-AMNE

Selection of Oils, Surfactants, and Co-Surfactant for PO-AMNE Development

The selection of suitable components for the development of NE was determined in different components.

The solubility profiles of α -Mangostin in various components are depicted in Table 3, where the highest solubility of α -Mangostin was obtained in palm oil (29.579 ± 0.101 mg/mL), Tween 80 (70.804 ± 0.102 mg/mL), Span 80 (69.236 ± 0.032 mg/mL), and glycerol (212.412 ± 0.07 mg/mL). As a result, palm oil 90, Tween 80, Span 80, and glycerol were chosen as the oil, surfactant, and co-surfactant for the next phase of NE development.

Table 3. Solubility profiles of α -Mangostin in different oils surfactants and co-surfactants.

| Oils | α -Mangostin Solubility * (mg/mL) |
|--------------------------------|--|
| Palm oil | 29.579 ± 0.101 |
| Olive | 27.288 ± 0.006 |
| Avocado | 27.38 ± 0.010 |
| Macadamia | 27.182 ± 0.011 |
| Almond | 27.885 ± 0.045 |
| Primrose | 26.807 ± 0.008 |
| Surfactants and Co-surfactants | α -Mangostin Solubility (mg/mL) * |
| Tween 80 | 70.804 ± 0.102 |
| Tween 20 | 64.31 ± 0.0588 |
| Lipophile | 34.71 ± 0.03 |
| Labrafac PG | 54.632 ± 0.014 |
| Labra CS | 64.104 ± 0.074 |
| Peceol | 39.2422 ± 0.25 |
| Maisine | 34.51 ± 0.045 |
| Glycerol | 212.412 ± 0.07 |
| Transcutol HP | 418.457 ± 0.122 |
| Transcutol HP | 417.755 ± 0.076 |
| Span 80 | 69.236 ± 0.032 |

* The data are presented in this table as the mean \pm SD, $n = 3$.

3.2. Measurement of Droplet Size, Polydispersity Index, and Zeta Potential

3.2.1. Droplet Size

Among the various physical properties of nano-emulsion, droplet size is one of the most crucial parameters because it affects the formulation aesthetic appeal and stability [48]. To lessen the experimental burden, we included droplet size as one of the dependent

variables in the optimization procedure. Table 4 displays the results of a statistical analysis of the effect of the interaction between the percentage of oil, Smix, and glycerol (cosolvent) on the droplet size of blank nano-emulsion.

Table 4. Analysis of variance data for droplet size.

| Source | F-Ratio | <i>p</i> -Value |
|----------------|---------|-----------------|
| Model | 79.96 | <0.0001 |
| A | 568.47 | <0.0001 |
| B | 46.82 | 0.0002 |
| C | 0.0808 | 0.7845 |
| AB | 16.76 | 0.0046 |
| AC | 7.79 | 0.0269 |
| BC | 9.46 | 0.0179 |
| A ² | 48.02 | 0.0002 |
| B ² | 15.36 | 0.0058 |
| C ² | 8.53 | 0.0223 |
| Residual | | |
| Lack of Fit | 2.68 | 0.1823 |
| Pure Error | | |

The model F-value of 79.96 and *p*-value of <0.05 represented the significance of the best fit quadratic model, and the representative *p*-values (*p* < 0.05) for the model terms A, B, AB, AC, BC, A², B², and C² have the statistical significance influence on droplet size of the developed nano-emulsion.

The F-value of 2.68 and *p* > 0.05 for the lack of fit indicated the insignificance of the lack of fit relative to the pure error. Non-significance of the lack of fit is good as it represents the model to be fit. An adequate precision (signal-to-noise ratio) value of 28.764 indicated an adequate signal for the suggested quadratic model. Hence, this model could be used to navigate the design space. A polynomial equation on the responses of three independent variables on globule size was generated in the fitted model (Equation (2)), where Y1 represents the droplet size of the formulation. Coefficient values for the respective model terms help to identify the relative impact of the independent variables on globule size.

Together with increasing palm oil and glycerol %, the positive coefficient of model terms A (+230.71) and C (+2.75) represented that the droplet size of the nano-emulsion was also increased; although, the effect of glycerol content on the droplet size of the formulation was insignificant, as represented in Table 4 (*p* > 0.05). As per the literature, a significant effect of glycerol content was reported when the % of glycerol was more than 20% [49]. In our experiment, the percentage was within 20%, which might be the reason for the insignificant effect of glycerol content on droplet size. Alternatively, a negative coefficient value of −66.21 for the model term indicated increasing droplet size, with increasing % of Smix. The effect of oil content and Smix content on droplet size were in agreement with the literature data. The negative coefficient value (−56.02) of model term AB (Equation (2)) indicated decreasing in droplet size with increasing the combined effect of model terms A and B. Similarly, model term C was also associated with a negative coefficient, which represents a decrease in droplet size, with increasing combined interaction of model terms A and C. Combined effects of model terms AB and AC on droplet size were significant, which was evident in their respective *p*-values; whereas, a positive coefficient (+38.20) was associated with the model term AC, which represents the combined effect of model terms A and C as inverse with globule size.

$$Y1 = +428.76 + 230.71 \times A - 66.21 \times B + 2.75 \times C + 92.43 \times A^2 - 56.02 \times A \times B + 38.20 \times A \times C - 52.27 \times B^2 - 42.10 \times B \times C + 38.96 \times C^2 \quad (2)$$

Moreover, proportional increases in droplet size with increasing oil % are evident with a steep positive slope in the perturbation plot (Figure 1A) associated with increasing model term A, which is in agreement with the positive coefficient value (+230.71) of the model term A in Equation (2). Alternatively, the negative slope in the perturbation plot (Figure 1A) associated with increasing model term B indicated decreasing droplet size with increasing Smix %, which follows the negative slope (−66.21) of the model term B in Equation (2). The similar effect of model terms A and B are also evident in the 3D surface plot (Figure 1B). Increasing the surfactant % might provide a layer for the adsorption of the oil and water phase and reduce the interfacial tension between the dispersible droplets and the external aqueous phase, which leads to a decrease in droplet size [50]. Predicted and experimental globule size data are close together, which can be seen in the predicted vs. actual plot (Figure 1C).

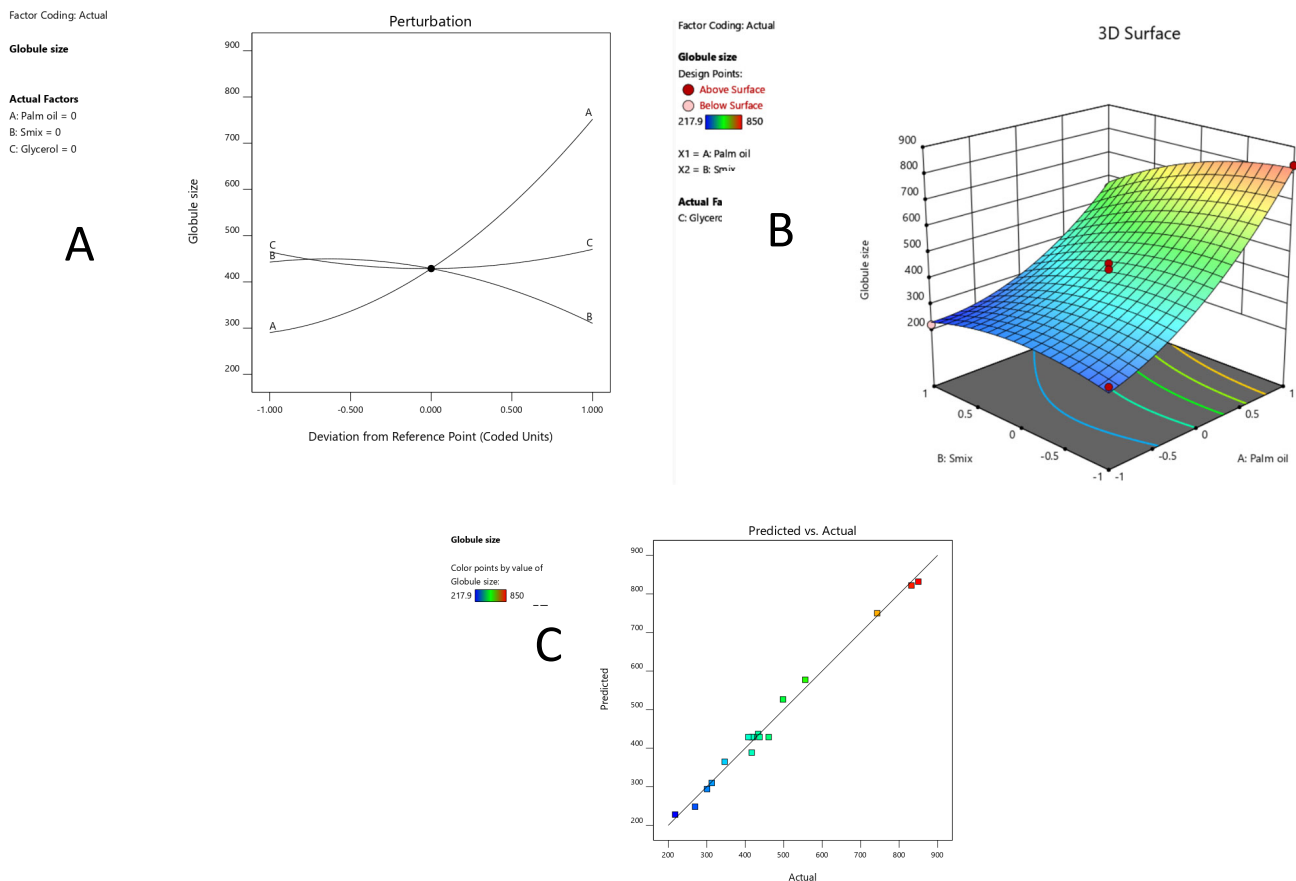


Figure 1. Effect of interaction of independent variables on the droplet size of nano-emulsion formulation: (A) Perturbation plot, (B) 3D surface plot, (C) predicted vs. actual graph.

3.2.2. Effect of the Independent Variable on Polydispersity Index

The PDI measures the homogeneity of dispersed oil droplets. Additionally, it ensures the formulation stability. Low PDI values signify the high kinetic stability of nano-emulsion formulation, while high PDI values signify low formulation stability [51]. Uniform droplets with a narrow size distribution are represented by low PDI values, which signify high kinetic stability.

The statistical data from the quadratic model, of the interaction of three independent variables on PDI, is mentioned in Table 5. The model F-value of 15.12 and p -value of 0.0008 ($p < 0.05$) indicated model significance. Further, model terms A, B, C, A^2 , and B^2 are found to have a significant effect on the PDI of the droplet size range of the formulation, as the respective $p < 0.05$. The F-value of 3.57 for the lack of fit term and respective p -value ($p > 0.05$) represented that the lack of fit is not significant relative to the pure error. An insignificant lack of fit is good, as we want the model to fit. Additionally, an adequate precision value of 14.113, more than 4, indicated a sufficient signal. Hence, this model could be used to navigate the design space.

Table 5. Analysis of variance data for PDI.

| Source | F-Ratio | p -Value |
|-------------|---------|------------|
| Model | 15.12 | 0.0008 |
| A | 19.96 | 0.0029 |
| B | 70.92 | <0.0001 |
| C | 7.34 | 0.0303 |
| AB | 1.72 | 0.2306 |
| AC | 0.3818 | 0.5562 |
| BC | 4.54 | 0.0705 |
| A^2 | 17.68 | 0.0040 |
| B^2 | 11.64 | 0.0113 |
| C^2 | 0.9561 | 0.3607 |
| Residual | | |
| Lack of Fit | 3.57 | 0.1254 |
| Pure Error | | |

The closeness of actual PDI and predicted PDI is evident in the predicted vs. actual plots (Figure 2C). The quadratic model generated a polynomial equation on the effect of three independent variables on the PDI of the formulation, presented in (Equation (3)), where Y_2 represents the PDI of the formulation. Coefficient values corresponding to the respective model terms indicate the relative impact of the independent variables on the PDI of the nano-emulsion.

$$Y_2 = +0.2396 + 0.0511 \times A - 0.0964 \times B + 0.0310 \times C + 0.0663 \times A^2 - 0.0212 \text{terms} - 0.0100 \times A \times C + 0.0538 \times B^2 - 0.0345 \times B \times C - 0.0154 \times C^2 \quad (3)$$

The positive coefficient of the model terms A and C, along with a significant p -value ($p < 0.05$) (Table 5 and Equation (3)), indicated the significant increase in PDI with increasing oil and glycerol % in nano-emulsion; whereas the negative coefficient value associated with the model term B indicated that there was a decrease in PDI with increasing surfactant content. The perturbation plot and 3D surface plot on the effect of % of oil, Smix, and glycerol on PDI of the formulation, are shown in Figure 2A,B, respectively, where an increasing PDI with increasing oil content, and contrarily, the decreasing PDI with increasing Smix, is evident. The obtained results are in agreement with the respective negative and positive coefficient values in Equation (3). Additionally, the highest coefficient value associated with the model term B was also reflected with a sharp negative decline in the perturbation plot with model term B. The positive coefficient value of A was reflected in the positive slope associated with model term A in the perturbation plot, whereas the least coefficient value associated with model term C in Equation (3) was also related to model term C in Table 5 and the smallest slope in the perturbation plot, per the insignificant p -value (Figure 2C).

Increasing the amount of surfactant may result in the successful coating of oil droplets, which may result in a low PDI value. In addition, as the number of oil droplets increases,

there may be insufficient surfactant to effectively coat the dispersed droplets in nano-emulsion formulation, leading to the coalescence of incompletely coated dispersed droplets. Our findings are consistent with the published literature [51].

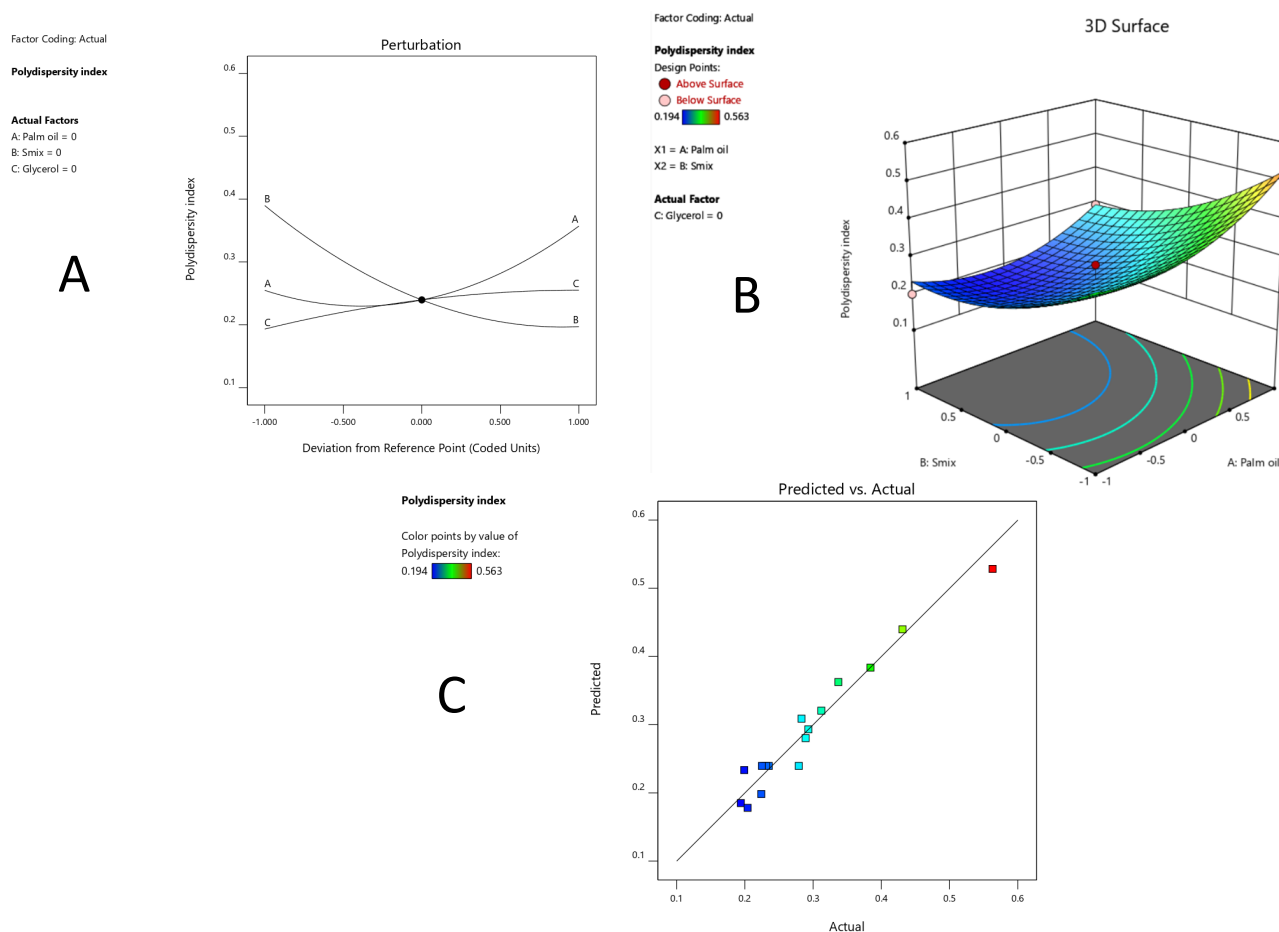


Figure 2. Effect of independent variables on PDI: (A) Perturbation graph of the droplet size, (B) 3D surface plot, (C) predicted vs. actual graph.

3.3. Optimization and Characterization of 0.2% PO-AMNE

α -Mangostin was loaded into the optimized NE formulation by dissolving the drug to obtain a final concentration of 0.2% mg/mL (20 mg/mL) in the oil phase, and formulated as described above, incorporating desired percentages of Smix and the aqueous phase. The globule size of the drug-loaded NE was determined as 340.9 nm, whereas the PDI 0.246 and surface charge were recorded as 27.2 ± 0.7 mV (Figure 3). α -Mangostin was loaded into the optimized NE formulation by dissolving the drug to achieve a final concentration of 0.2% mg/mL (20 mg/mL) in the oil phase and formulating with the desired proportions of Smix and the aqueous phase, as described above. The globule size of the drug-loaded NE was measured to be 340.9 nm, while the PDI 0.246 and surface charge were measured to be -27.2 ± 0.7 mV, respectively (Figure 3b).

The 0.2% PO-AMNE was formulated using concentrations of 0.2% α -Mangostin solution, and the formulation was then characterized based on the change in globule size, PDI, and surface charge. TEM analysis of the 0.2% PO-AMNE formulation revealed the coated droplets' spherical morphology (Figure 3A). Figure 3B histogram indicates that the particles in the PO-AMNE formulation have a smaller range of sizes, which is consistent with Table 6 PDI value (0.246) and the morphological observation in the TEM image (Figure 3B). In addition, the uniformity of the droplet size (340.9 nm) in the absence of crystalline AM confirmed that the drug was completely entrapped within the oil phase of the formulation.

Table 6. Physical characterization of 0.2% PO-AMNE.

| Nano-Formulation | Average Particle Size (nm) | Polydispersity Index (PDI) | Zeta Potential (mV) |
|------------------|----------------------------|----------------------------|---------------------|
| 0.2% PO-AMNE | 340.9 nm | PDI 0.246 | -27.2 ± 0.7 mV |

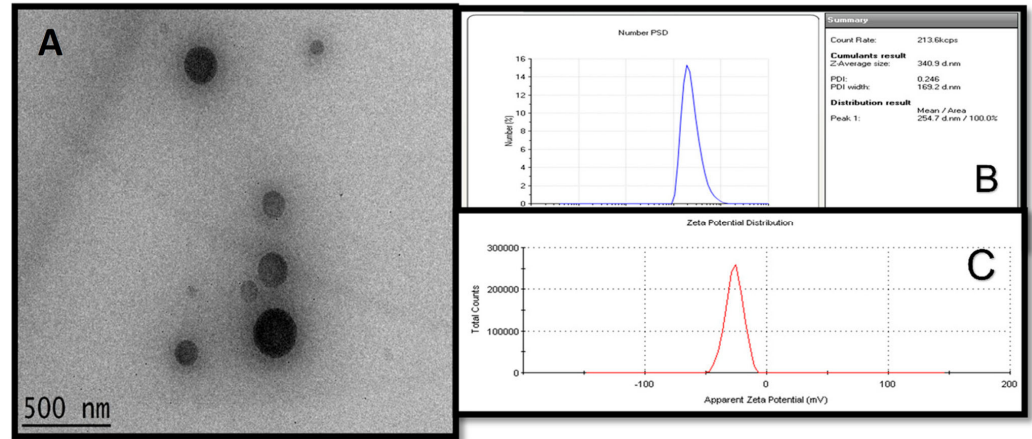


Figure 3. Representation of morphology of the optimized (0.2%) PO-AMNE (A), particle size distribution (B), and zeta potential (C).

3.4. Ex Vivo Antimicrobial Studies

3.4.1. Enumeration and Identification of *Enterococcus Faecalis*, *Staphylococcus epidermidis*, and *Candida albicans*

For the identification of any metabolic alterations for three test organisms, *E. faecalis*, *S. epidermidis*, and *C. albicans*, an analytical profile index (API) identification scheme was used (Figure 4A–C).

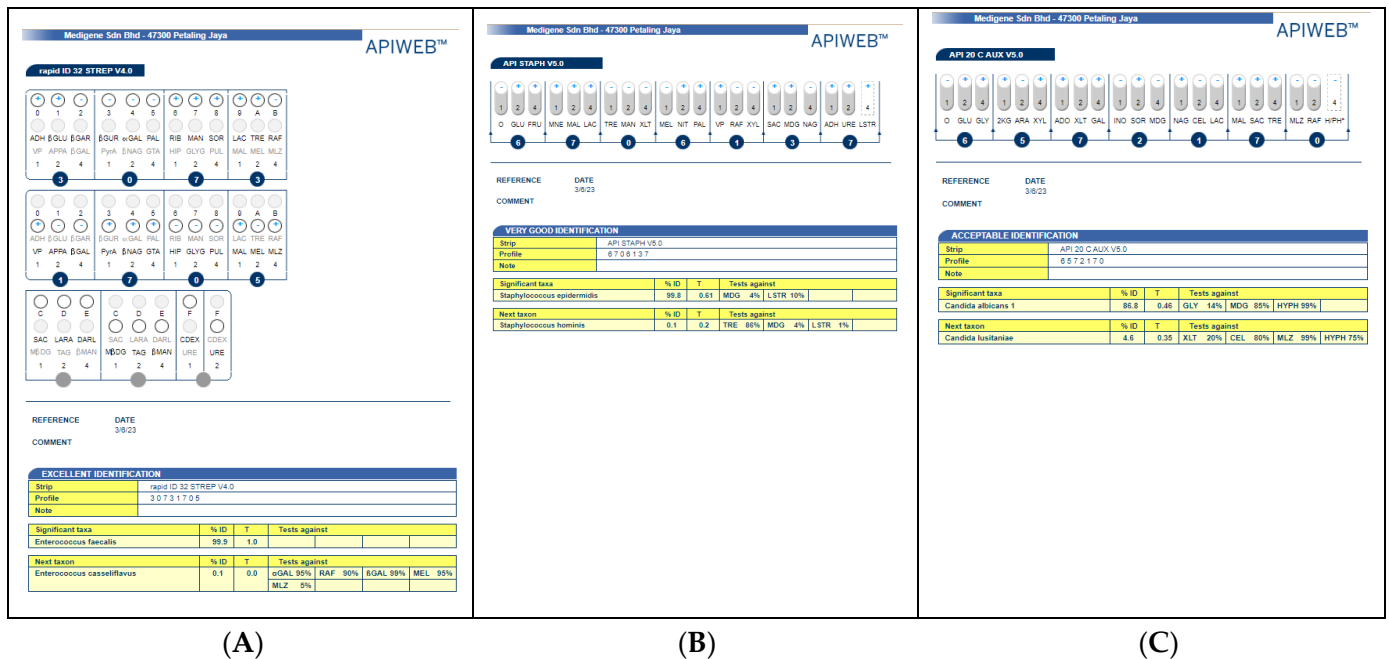


Figure 4. (A) API identification of *E. faecalis*; (B) API identification of *S. epidermidis*; (C) API identification of *C. albicans*.

3.4.2. Determination of Minimum Inhibitory Concentration (MIC)

α -Mangostin is comparable to both 3.25% NaOCl and 2% CHX in inhibiting the growth of tested microbes. The MIC values showed that 0.2% α -Mangostin (1.22 ± 0.02) was comparable to 2% CHX (1.33 ± 0.01) and 3.25% NaOCl (2.2 ± 0.09) and had the least inhibition of *E. faecalis*. NaOCl (3.25%) showed the maximum inhibition of *S. epidermidis* (0.26 ± 0.05), whereas 0.2% α -Mangostin (1.25 ± 0.0) was comparable to 2% CHX (1.86 ± 0.07). For *C. albicans*, 2% CHX (8.12 ± 0.12) showed the least inhibition, as compared to 0.2% α -Mangostin (1.23 ± 0.02) and 3.25% NaOCl (0.59 ± 0.02), as shown in Figure 5.

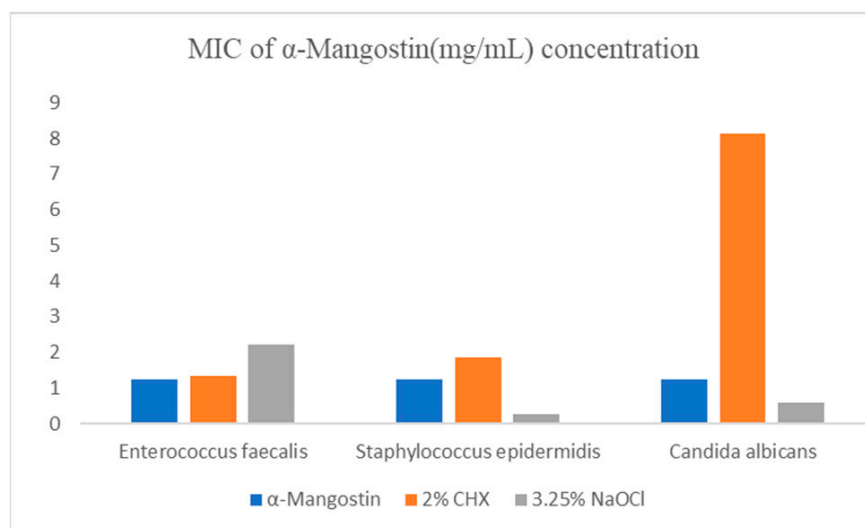


Figure 5. MIC of α -Mangostin(mg/mL) concentration against *E. faecalis*, *S. epidermidis*, and *C. albicans*.

3.5. Ex Vivo Experiment: Preparation of Human Teeth Specimens to Check the Antimicrobial Efficacy of PO-AMNE Irrigant in a Tooth Model Using Colony-Forming Units (CFU)

3.5.1. Antimicrobial Assessment Using CFU

A reduction in the number of CFUs was statistically significant in all groups compared to the control group ($p < 0.05$).

Results for *E. faecalis* at 200 μ m

The mean CFU of 0.2% PO-AMNE was 4.63 ± 0.26 , 4.68 ± 0.35 for 2% CHX, 4.87 ± 0.15 for 3.25% NaOCl, and 6.05 ± 0.04 for saline, as shown in Table 7. In the presence of nano-formulation, the CFU formation of *E. faecalis* was lower compared to either 2% CHX or 3.25% NaOCl at a depth of 200 μ m, showing its potent antimicrobial effect.

Table 7. Mean and standard deviation of irrigants against *E. faecalis* at 200 μ m.

| Irrigants | N | Mean | Std. Deviation |
|--------------|----|------------|----------------|
| 0.2% PO-AMNE | 10 | 4.63972392 | 0.266228615 |
| 2% CHX | 10 | 4.68676222 | 0.350818870 |
| 3.25% NaOCl | 10 | 4.87883986 | 0.158879880 |
| Saline | 10 | 6.05010073 | 0.043594317 |
| Total | 40 | 5.06385668 | 0.625931661 |

Overall, 0.2% PO-AMNE had statistical significance when compared to 2% CHX against *E. faecalis*. The 95% confidence interval was -0.2455 to 0.3396 , with a standard error of 0.139 . The p -value was found to be <0.0001 . Similarly, the 0.2% PO-AMNE irrigant had statistical significance when compared to 3.25% NaOCl. The 95% confidence interval was observed to be 0.0331 to 0.4451 , with a p -value of <0.0001 .

Results for *E. faecalis* at 400 μm

The mean CFU of 0.2% PO-AMNE was 5.20 ± 0.09 , 5.52 ± 0.07 for 2% CHX, 5.52 ± 0.27 for 3.25% NaOCl and 6.14 ± 0.01 for saline, as shown in Table 8. In the presence of nano-formulation, the CFU formation of *E. faecalis* was lower when compared to either CHX or NaOCl at a depth of 400 μm , showing its potent antimicrobial effect.

Table 8. Mean and standard deviation of irrigants against *E. faecalis* at 400 μm .

| Irrigants | N | Mean | Std. Deviation |
|--------------|----|------------|----------------|
| 0.2% PO-AMNE | 10 | 5.20722816 | 0.098434833 |
| 2% CHX | 10 | 5.52280850 | 0.074578498 |
| 3.25% NaOCl | 10 | 5.52824399 | 0.027822768 |
| Saline | 10 | 6.14335492 | 0.016507675 |
| Total | 40 | 5.60040889 | 0.349093792 |

Overall, 0.2% PO-AMNE had statistical significance when compared to 2% CHX against *E. faecalis*. The 95% confidence interval was -0.3976 to -0.2335 , with a standard error of 0.039. The *p*-value was found to be <0.0001 . Similarly, the 0.2% PO-AMNE irrigant had statistical significance when compared to 3.25% NaOCl. The 95% confidence interval was observed to be 0.2531 to 0.3890, with a *p*-value of <0.0001 .

Results for *S. epidermidis* at 200 μm

The mean CFU of 0.2% PO-AMNE was 3.77 ± 0.37 , 4.44 ± 0.34 for 2%, 4.78 ± 0.86 for 3.25% NaOCl and 6.07 ± 0.01 for saline, as shown in Table 9. In the presence of nano-formulation, the CFU of *S. epidermidis* was lower when compared to either CHX or NaOCl at a depth of 200 μm , showing its potent antimicrobial effect.

Table 9. Mean and standard deviation of irrigants against *S. epidermidis* at 200 μm .

| Irrigants | N | Mean | Std. Deviation |
|--------------|----|------------|----------------|
| 0.2% PO-AMNE | 10 | 3.77083657 | 0.379532943 |
| 2% CHX | 10 | 4.44137166 | 0.342868124 |
| 3.25% NaOCl | 10 | 4.78653050 | 0.086264246 |
| Saline | 10 | 6.07355352 | 0.013985945 |
| Total | 40 | 4.76807306 | 0.884068563 |

Overall, 0.2% PO-AMNE had statistical significance when compared to 2% CHX against *E. faecalis*. The 95% Confidence interval was 0.3307 to 1.0103, with a standard error of 0.162. The *p*-value was found to be <0.0001 . Similarly, the 0.2% PO-AMNE irrigant had statistical significance when compared to 3.25% NaOCl. The 95% confidence interval was observed to be 0.7571 to 1.2743, with a *p*-value of <0.0001 .

Results for *S. epidermidis* at 400 μm

The mean CFU of 0.2% PO-AMNE was 4.40 ± 0.17 , 4.54 ± 0.14 for 2% CHX, 5.00 ± 0.29 for 3.25% NaOCl and 6.13 ± 0.01 for saline, as shown in Table 10. In the presence of nano-formulation, the CFU formation of *S. epidermidis* was lower when compared to either CHX or NaOCl at a depth of 400 μm , showing its potent antimicrobial effect.

Table 10. Mean and standard deviation of irrigants against *S. epidermidis* at 400 μm .

| Irrigants | N | Mean | Std. Deviation |
|--------------|----|-------------|----------------|
| 0.2% PO-AMNE | 10 | 0.171520772 | 0.054239631 |
| 2% CHX | 10 | 0.469422690 | 0.148444489 |
| 3.25% NaOCl | 10 | 0.094514831 | 0.029888214 |
| Saline | 10 | 0.016537682 | 0.005229674 |
| Total | 40 | 0.731541254 | 0.115666828 |

Overall, 0.2% PO-AMNE had statistical significance when compared to 2% CHX against *S. epidermidis*. The 95% confidence interval was -0.1951 to 0.4690 , with a standard error of 0.158 . The *p*-value was found to be <0.0001 . Similarly, the 0.2% PO-AMNE irrigant had statistical significance when compared to 3.25% NaOCl. The 95% confidence interval was observed to be 0.4658 to 0.7260 , with a *p*-value of <0.0001 .

Results for *C. albicans* at 200 μm

The mean CFU of 0.2% PO-AMNE was $2.83 + 0.24$, 3.14 ± 0.18 for 2%CHX, 3.34 ± 0.24 for 3.25% NaOCl and 5.09 ± 0.02 for saline, as shown in Table 11. In the presence of nano-formulation, the CFU formation of *C. albicans* was lower when compared to either CHX or NaOCl at a depth of 200 μm , showing its potent antimicrobial effect.

Table 11. Mean and standard deviation of irrigants against *C. albicans* at 200 μm .

| Irrigants | N | Mean | Std. Deviation |
|--------------|----|------------|----------------|
| 0.2% PO-AMNE | 10 | 2.83659430 | 0.247612845 |
| 2% CHX | 10 | 3.14848172 | 0.181043992 |
| 3.25% NaOCl | 10 | 3.34090591 | 0.240291718 |
| Saline | 10 | 5.09852677 | 0.020267240 |
| Total | 40 | 3.60612717 | 0.910935697 |

Overall, 0.2% PO-AMNE had statistical significance when compared to 2% CHX against *C. albicans*. The 95% confidence interval was 0.1081 to 0.5157 , with a standard error of 0.097 . The *p*-value was found to be <0.0001 . Similarly, the 0.2% PO-AMNE irrigant had statistical significance when compared to 3.25% NaOCl. The 95% confidence interval was observed to be 0.2751 to 0.7335 , with a *p*-value of <0.0001 .

Results for *C. albicans* at 400 μm

The mean CFU of 0.2% PO-AMNE was 2.95 ± 0.15 , 3.11 ± 0.14 for 2% CHX, 3.33 ± 0.11 for 3.25% NaOCl and 5.14 ± 0.02 for saline, as shown in Table 12. In the presence of nano-formulation, the CFU formation of *C. albicans* was lower when compared to either CHX or NaOCl at a depth of 400 μm , showing its potent antimicrobial effect.

Overall, 0.2% PO-AMNE had statistical significance when compared to 2% CHX against *C. albicans*. The 95% confidence interval was 0.0143 to 0.2965 , with a standard error of 0.067 . The *p*-value was found to be <0.0001 . Similarly, the 0.2% PO-AMNE irrigant had statistical significance when compared to 3.25% NaOCl. The 95% confidence interval was observed to be 0.2559 to 0.4978 , with a *p*-value of <0.0001 .

Table 12. Mean and standard deviation of irrigants against *C. albicans* at 400 µm.

| Irrigants | N | Mean | Std. Deviation |
|--------------|----|------------|----------------|
| 0.2% PO-AMNE | 10 | 2.95885666 | 0.150876977 |
| 2% CHX | 10 | 3.11424553 | 0.149477061 |
| 3.25% NaOCl | 10 | 3.33568568 | 0.101826728 |
| Saline | 10 | 5.14021700 | 0.025604369 |
| Total | 40 | 3.63725122 | 0.896448891 |

3.6. Smear Layer Removal in Tooth Models

The results obtained from this study are summarized in Tables 13–15, and show the SEM images (Figure 6) of the tested irrigants. Group 1: 0.2% PO-AMNE and group 2: 17% EDTA exhibited better efficacy in removing the smear layer without altering the normal dentinal structures with the lowest mean scores ($p < 0.001$), followed by group 3: saline. For all the treated groups, there was no statistically significant difference ($p < 0.05$) between the scores at each root third (cervical, middle, apical).

Table 13. Group 1: Debris score with 0.2% PO-AMNE.

| Coronal Third | | | | | Middle Third | | | | | Apical Third | | | | |
|---------------|------|----------------|---|---|--------------|------|----------------|---|---|--------------|------|----------------|------|---|
| Clean | | Debris Present | | | Clean | | Debris Present | | | Clean | | Debris Present | | |
| 1* | 2 | 3 | 4 | 5 | 1 | 2 | 3 | 4 | 5 | 1 | 2 | 3 | 4 | 5 |
| 0 | 8/10 | 2/10 | 0 | 0 | 1/10 | 8/10 | 0 | 0 | 0 | 0/10 | 8/10 | 1/10 | 1/10 | 0 |
| + | | + | | | + | | + | | | + | | + | | |
| 8/10 + | | 2/10 + | | | 9/10 + | | 0/10 + | | | 8/10 + | | 2/10 + | | |
| (80%)*+ | | (20%)*+ | | | (30%)*+ | | (70%)*+ | | | (60%)*+ | | (100%)*+ | | |

* Debris scores (Hülsmann et al., 1997 [45]). + Number of canals presented with a given score. *+ Dichotomized scores: scores 1 to 2 (clean canal wall) versus 3 to 5 (debris present).

Table 14. Group 2: Debris score with 17% EDTA.

| Coronal Third | | | | | Middle Third | | | | | APICAL THIRD | | | | |
|---------------|------|----------------|---|---|--------------|------|----------------|---|---|--------------|------|----------------|-------|---|
| Clean | | Debris Present | | | Clean | | Debris Present | | | Clean | | Debris Present | | |
| 1* | 2 | 3 | 4 | 5 | 1 | 2 | 3 | 4 | 5 | 1 | 2 | 3 | 4 | 5 |
| 0 | 8/10 | 2/10 | 0 | 0 | 0 | 4/10 | 6/10 | 0 | 0 | 1/0 + | 4/10 | 2/10 | 1/0 + | 0 |
| + | | + | | | + | | + | | | + | | + | | |
| 8/10 + | | 2/10 + | | | 4/10 + | | 6/10 + | | | 5/10 + | | 3/10 + | | |
| (100%)*+ | | (100%)*+ | | | (100%)*+ | | (100%)*+ | | | (100%)*+ | | (100%)*+ | | |

* Debris scores (Hülsmann et al., 1997 [45]). + Number of canals presented with a given score. *+ Dichotomized scores: scores 1 to 2 (clean canal wall) versus 3 to 5 (debris present).

Table 15. Group 2: Debris score with saline.

| Coronal Third | | | | | Middle Third | | | | | Apical Third | | | | |
|---------------|---|----------------|---|-------|--------------|---|----------------|---|-------|--------------|---|----------------|---|-------|
| Clean | | Debris Present | | | Clean | | Debris Present | | | Clean | | Debris Present | | |
| 1* | 2 | 3 | 4 | 5 | 1 | 2 | 3 | 4 | 5 | 1 | 2 | 3 | 4 | 5 |
| 0 | 0 | 0 | 0 | 10/10 | 0 | 0 | 0 | 0 | 10/10 | 0 | 0 | 0 | 0 | 10/10 |
| + | | + | | | + | | + | | | + | | + | | |
| 0/10 + | | 10/10 + | | | 0/10 + | | 10/10 + | | | 0/10 + | | 10/10 + | | |
| (100%)*+ | | (100%)*+ | | | (100%)*+ | | (100%)*+ | | | (100%)*+ | | (100%)*+ | | |

* Debris scores (Hülsmann et al., 1997 [45]). + Number of canals presented with a given score. *+ Dichotomized scores: scores 1 to 2 (clean canal wall) versus 3 to 5 (debris present).

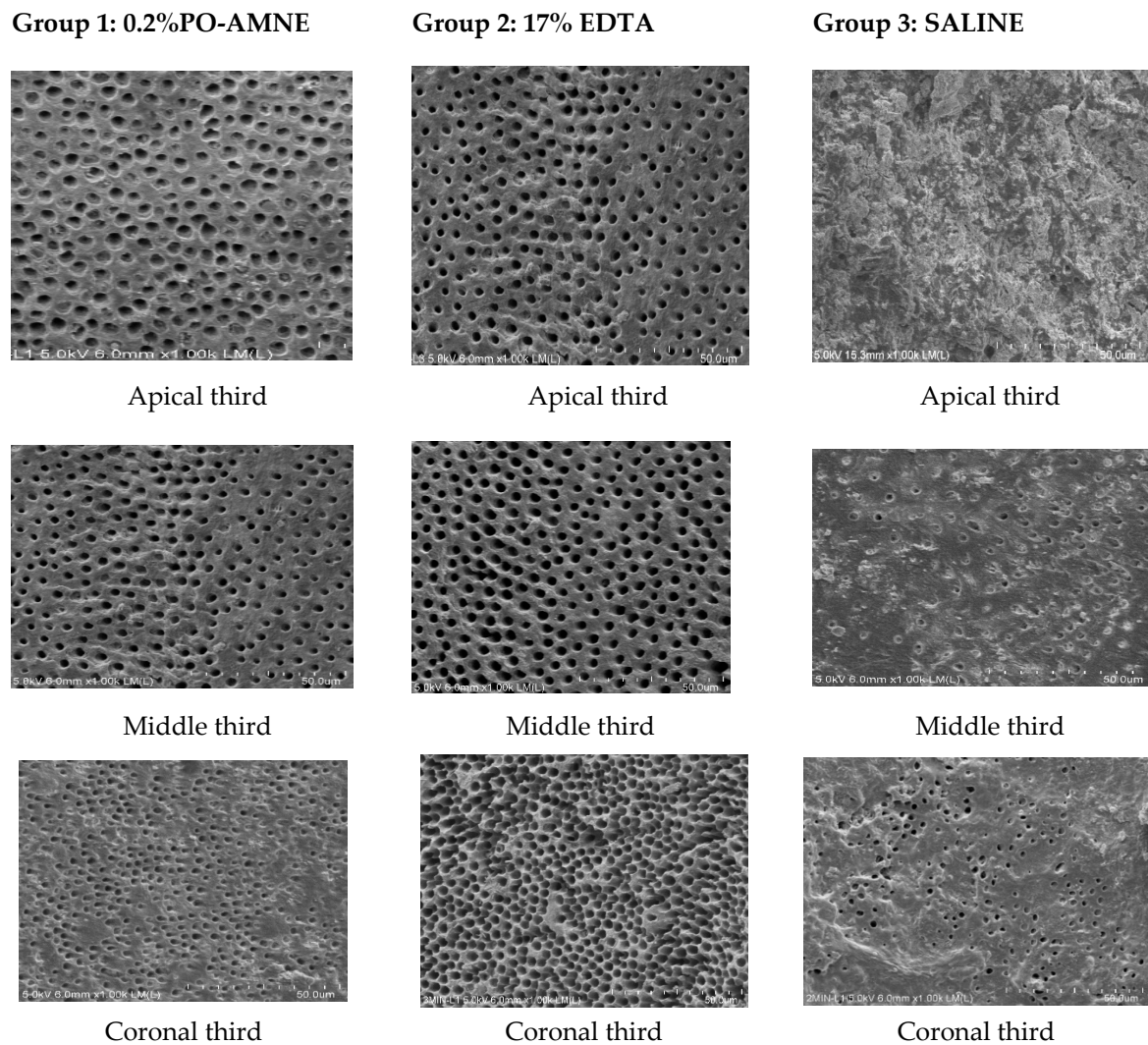


Figure 6. SEM images of all groups.

3.6.1. Debris Scores for 0.2% PO-AMNE

In the coronal third, 8 out of 10 (80%) samples were scored as 2, respectively, representing a clean dentin surface. In the middle third, 9 out of 10 (90%) were scored 1 or 2, respectively, representing a clean dentin surface, and 0 out of 10 (60%) were scored as 3, 4, and 5. In the apical third, 8 out of 10 (80%) samples were scored as 2, representing a clean dentin surface, and 2 out of 10 (20%) samples were scored as 3 and 4, respectively, representing debris present on the dentin surface, as shown in Table 13.

3.6.2. Debris Scores for 17% EDTA

In the coronal third, 8 out of 10 (80%) and 2 out of 10 (20%) samples were scored as either 1 or 2, respectively, representing a clean dentin surface. In the middle third, 4 out of 10 (40%) were scored as 2, representing a clean dentin surface, and 6 out of 10 (60%) were scored as 3, respectively, representing debris present on the dentin surface. In the apical third, 5 out of 10 (50%) samples were scored as either 1 or 2, respectively, representing a clean dentin surface, and 5 out of 10 (50%) samples were scored as either 3, 4 or 5, respectively, representing debris present on the dentin surface, as shown in Table 14.

3.6.3. Debris Score for Saline

In the coronal third, no samples were characterized with scores of 1 or 2, and 10 out of 10 (100%) samples were scored as 5, representing debris present on the dentin surface.

In the middle third, no samples were characterized with scores of 1 or 2, and 10 out of 10 (100%) samples were scored as 5, representing debris present. In the apical third, 0 out of 10 (100%) samples were scored as either 1 nor 2, and 10 out of 10 canals (100%) were scored as 5, representing debris present on the dentin surface as shown in Table 15.

Group 1 (0.2%) PO-AMNE and group 2 (17% EDTA) exhibited better efficacy in removing the smear layer without altering the normal dentinal structures with the lowest mean scores ($p < 0.001$), followed by group 3 (saline). There was no statistically significant difference ($p < 0.05$) between the scores at each root third (cervical, middle, apical) for group 1 and group 2, though the apical third scores were less than the other root thirds.

3.7. Biocompatibility Test Using Alamar Blue Assay on Immortalized Oral Keratinocytes OKF-6 Cells

The proliferation percentage of the OKF-6 cells in the presence of various irrigants is presented in Figure 7. The percentage of OKF-6 cells was calculated at 1 min, 5 min, 10 min, 30 min, and 60 min. The results show that group 1 (20 mg α -Mangostin) was comparable to group 2 (0.2% PO-AMNE) after 60 min, with cell viability percentages of 35.48% and 32.51%, whereas there was a decrease in the cell viability percentages for group 3 (3.25% NaOCl), group 4 (CHX), and group 5 (17% EDTA) proliferation percentages of 6.47%, 4.30%, and 4.15%, respectively.

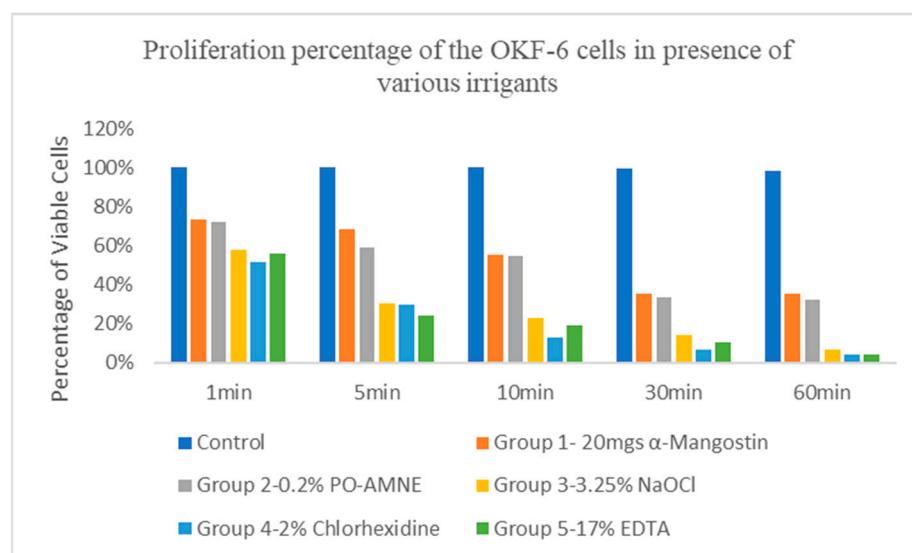


Figure 7. Proliferation percentage of OKF-6 cells in the presence of various irrigants.

4. Discussion

For many years, root canal irrigants have been utilized as an adjuvant to improve the antibacterial efficacy of endodontic cleaning and shaping. Because of its pulp-dissolving and antibacterial properties, NaOCl is the most used irrigant for treating infected root canals. However, when injected into the periapical tissues, it has a cytotoxic effect, leaves a bad odor and taste, has a corrosive potential, and may cause allergic reactions. Due to its extensive antibacterial action, the cationic bis-biguanide CHX has been employed as an irrigating solution during root canal therapy. However, the use of CHX as a root canal irrigant is limited, because it has no tissue solvent activity and some patients may have allergic reactions to it; additionally, it can discolor teeth [52]. A previous study has shown that both NaOCl and CHX impair the mitochondrial activity of human periodontal ligament (PDL) cells, making them extremely cytotoxic [53]. As a result, there is a growing need for irrigants with effective antimicrobial properties, that are also biocompatible with oral tissues.

The filling of the dentinal walls and organic remnants present in the canal leaves an uneven and granular smear layer during root canal instrumentation, called the smear

layer [54]. This layer obstructs the dentinal tubules by reducing dentinal permeability, delaying the action of topical medications and irrigants, and preventing close contact of the filling material with the dentinal walls [55]. Consequently, there is a greater chance of bacterial infection and failure. The choice of commercially available chelating agents used in the study was EDTA and citric acid for smear layer removal, as there are ample data in the literature showing the effectiveness of these agents for the elimination of the smear layer from root canals. Citric acid is a weak acid that removes the smear layer, has strong chemical stability, is inexpensive, and has excellent results [56].

The selection of *E. faecalis*, *C. albicans*, and *S. epidermidis* biofilms was based on scientific data demonstrating that these pathogens are the most often isolated bacterial species in endodontic patients. *E. faecalis* in dentinal tubules is 1000 times more resistant to phagocytosis, antibodies, and antimicrobials than non-biofilm-producing organisms. Additional virulence features have been observed in *E. faecalis* clinical isolates from asymptomatic, chronic endodontic infections of the root canal and oral cavity [57]. *C. albicans* has been regularly identified as the species most often recovered from failing root canals requiring retreatment. Waltimo et al. proposed fungi as microorganisms resistant to endodontic therapy in apical periodontitis and proved that *C. albicans* species need incubation with a saturated calcium hydroxide solution for 16 h [58]. Peciuliene et al. [59] identified fungi as resistant microorganisms in the obturated root canals of teeth diagnosed with chronic apical periodontitis. Egan et al. conducted a study to determine the association between the presence of fungi in the saliva and the root canals of teeth in patients with apical periodontitis. They discovered that fungi were 13.8 times more prevalent in the root canals when they were also present in the patient's saliva [60].

The Gram-positive bacterium, *S. epidermidis*, was frequently found to be the cause of endodontic flare-ups and secondary infections. However, in many instances, the infection has persisted despite multiple attempts to alleviate symptoms (such as intracanal medication placement and antimicrobials) [61].

Our study aimed to formulate an oil-based nano-emulsion containing a mixture of α -Mangostin, palm oil, Tween[®] 80, Span[®] 80, glycerol, and 10% citric acid and investigate its effectiveness at inhibiting *E. faecalis*, *S. epidermis*, and *C. albicans* biofilms, as well as to assess its biocompatibility using immortalized oral keratinocyte (OKF-6) cells.

In our study, the solubility profiles of α -Mangostin in various oils, such as olive oil, macadamia oil, almond oil, and primrose oil, were evaluated. The highest solubility of AM was obtained with palm oil (29.57 mg/mL), Tween[®] 80 (70.80 mg/mL), Span[®] 80 (69.23 mg/mL), and glycerol (212.41 mg/mL). As a result, palm oil 90, Tween[®] 80, Span[®] 80, and glycerol were the oils, surfactants, and co-surfactants of choice for the next phase of NE development. Based on the Box–Behnken statistical design, the composition of nano-emulsion 0.2% PO-AMNE had an average particle size of 340.9 nm. This was in agreement with studies conducted by Marcel et al., who developed a limonene nano-emulsion formed by a high-pressure homogenizer. The average particle size in their study varied from 264.50 nm to 434.20 nm [62]. The zeta potential is used for predicting dispersion stability, and its value depends on the physicochemical property of the drug, polymer, vehicle, presence of electrolytes, and adsorption. The zeta potential of 0.2% PO-AMNE in this study was -27.2 ± 0.7 mV. It is in accordance with a study done by Đorđević et al., who concluded that a zeta potential of ± 30 mV is sufficient to ensure the physical stability of NE [63]. Ahmad et al. concluded that all their nano-formulations had a zeta potential of -28.5 to -40.2 mV. The formulations having a zeta potential charge value greater than -30 mV indicate that nano-emulsion formulations are stable [64]. The PDI represents the consistency of nano-emulsion droplet size. The greater the value, the less uniform the nano-emulsion droplet size will be. It is the ratio of the standard deviation to the mean droplet size. A PDI of 0.08 or less indicates a monodispersed sample, while 0.08 to 0.70 represents the middle range of PDI [65]. Our research revealed a PDI of 0.246, which showed the consistency of nano-emulsion droplet sizes.

The MIC values in our study showed that 0.2% α -Mangostin (1.22 ± 0.02) was comparable to 2% CHX (1.33 ± 0.01) and 3.25% NaOCl (2.2 ± 0.09) for *E. faecalis*. These results were consistent with the study by Kaomongkolgit et al., which showed that α -Mangostin is effective against *E. faecalis* [66]. In our study, 3.25% NaOCl showed maximum inhibition of *S. epidermidis* (0.26 ± 0.05), whereas 0.2% α -Mangostin (1.25 ± 0.00) was comparable to 2% CHX (1.86 ± 0.07), in accordance with Sivaranjani et al. [67]. For *C. albicans*, 2% CHX (8.12 ± 0.12) showed the least inhibition as compared to 0.2% α -Mangostin (1.23 ± 0.02) and 3.25% NaOCl (0.59 ± 0.02), as per the results reported by Kaomongkolgit et al., who determined that α -Mangostin's potent antifungal activity and low toxicity made it a viable drug for the treatment of oral candidiasis [68]. The irrigant 0.2% PO-AMNE was bactericidal and fungicidal against *E. faecalis*, *S. epidermidis*, and *C. albicans* biofilms. According to a study by Leelapornpisid et al., the planktonic inhibitory concentrations of α -Mangostin were bactericidal on *E. faecalis* at 2–4 mg/L, and candidal on *C. albicans* at 1000 mg/L [69]. We discovered that 0.2% PO-AMNE was both bactericidal and fungicidal against *E. faecalis*, *S. epidermidis*, and *C. albicans* biofilms at 0.625 mg/L, which is lower than previously published literature [69]. Our results are in agreement with the study by Nourzadeh et al., where the mean CFU of 0.2% PO-AMNE (4.63 ± 0.26) was lower than for 2% CHX (4.68 ± 0.35), 3.25% NaOCl (4.87 ± 0.15) and saline (6.05 ± 0.04) at a depth of 200 μm for *E. faecalis*. The same findings were observed at a depth of 400 μm , where the mean CFU of 0.2% PO-AMNE (5.20 ± 0.09) was lower than 2% CHX (5.52 ± 0.07), 3.25% NaOCl (5.52 ± 0.27) and saline (6.14 ± 0.01) [70]. Overall, 0.2% PO-AMNE had a statistically significant difference when compared to 2% CHX and 3.25% NaOCl against *E. faecalis* at 200 μm and 400 μm .

The mean CFU in our study for *S. epidermidis*, at a depth of 200 μm , was 3.77 ± 0.37 for 0.2% PO-AMNE, 4.44 ± 0.34 for 2% CHX, 4.78 ± 0.86 for 3.25% NaOCl and 6.07 ± 0.01 for saline. At a depth of 400 μm , the mean CFU of *S. epidermidis* was 4.40 ± 0.17 for 0.2% PO-AMNE, 4.54 ± 0.14 for 2% CHX, 5.00 ± 0.29 for 3.25% NaOCl and 6.13 ± 0.01 for saline. Overall, 0.2% PO-AMNE had statistical significance when compared to 2% CHX and 3.25% NaOCl against *S. epidermidis* at 200 μm and 400 μm . The CFU formation at a depth of 200 μm and 400 μm for *S. epidermidis* in the presence of 0.2% PO-AMNE was lower when compared to either 2% CHX or 3.25% NaOCl, showing its potent antimicrobial effect. The overall results for *S. epidermidis* at 200 and 400 μm were in agreement with the study done by Schmidt et al., who studied the effects of CHX, povidone-iodine, and triple antibacterial solution against *S. epidermidis* biofilms [71].

In our study, the mean CFU of 0.2% PO-AMNE (2.83 ± 0.24) was lower than 2% CHX (3.14 ± 0.18), 3.25% NaOCl (3.34 ± 0.24) and saline (5.09 ± 0.02), at a depth of 200 μm for *C. albicans*. The same results were observed at a depth of 400 μm , where the mean CFU of 0.2% PO-AMNE (2.95 ± 0.15) was lower than 2% CHX (3.11 ± 0.14), 3.25% NaOCl (3.33 ± 0.11) and saline (5.14 ± 0.02). This shows that 0.2% PO-AMNE has a potent anti-fungal effect. This is in accordance with the study conducted by Vianna et al., 2004, who evaluated the in vitro antifungal activity of CHX and NaOCl. They concluded that CHX eliminated *C. albicans* within 15 s [72]. Radcliffe et al. tested the effects of various concentrations of NaOCl on *C. albicans* and found that all concentrations of NaOCl reduced CFU below the limit of detection within 10 s [73].

In our study, the SEM analysis showed that none of the tested root canal irrigants could completely remove the smear layer. According to our study, 0.2% PO-AMNE and 17% EDTA exhibited better efficacy in removing the smear layer without altering the normal dentinal structures with the lowest mean scores ($p < 0.001$), followed by saline. There was no statistically significant difference ($p < 0.05$) between the scores at each root third (cervical, middle, apical) for all groups. This is per the findings by Sakinah et al., who concluded that the results of SEM photomicrograph assessment showed a little debris on the surface of the root canal walls and plenty of opened dentin tubules on the canal walls irrigated with extract of mangosteen peel [74]. Charlie et al. reported similar results, where they concluded that EDTA might not penetrate the narrow apical region of teeth [75].

The oral keratinocyte cells were used for the study, as they act as the major barrier to physical, microbial, and chemical agents that may cause local cell injury [76]. They participate in the proinflammatory process by producing cytokines constitutively, or in response to a number of stimuli. Therefore, oral keratinocytes may contribute to the management of oral infections through an inflammatory process involving several interleukins, including IL-13 and IL-18 [77]. Oral mucosa keratinocytes are the primary source of IL-13, an inflammatory cytokine that regulates the production of IL-6 and IL-8 [78]. In our investigation, the proportion of OKF-6 cells proliferating in the presence of different irrigants was determined at 1 min, 5 min, 10 min, 30 min, and 60 min. According to our findings, 0.2% PO-AMNE had a better cell viability percentage of 32.51% after 60 min compared to 3.25% NaOCl, CHX, and 17% EDTA proliferation percentages, which decreased to 6.47%, 4.30%, and 4.15%, respectively. This is consistent with the studies done by Abate et al. and Ngawhirunpat et al., who found that *G. mangostana* extracts are not cytotoxic to human keratinocytes [79,80].

5. Conclusions

α -Mangostin from *Garcinia mangostana* Linn has been explored by many researchers and it has been observed that it is not just effective against bacteria, but also other microbes, such as fungi and mycobacteria. The optimization of the palm-oil-based α -Mangostin nano-emulsion (PO-AMNE) irrigant was performed using a Box–Behnken statistical design. The formulated 0.2% PO-AMNE endodontic irrigant had an overall significant antimicrobial effectiveness against *E. faecalis*, *S. epidermidis*, and *C. albicans* biofilms. 0.2% PO-AMNE endodontic irrigant was further evaluated for the smear layer removal and was found to be comparable with 17% EDTA. Finally, 0.2% PO-AMNE was found to be biocompatible with immortalized oral keratinocyte OKF-6 cells. Overall, the antimicrobial efficacy and safety of the formulated 0.2% PO-AMNE endodontic irrigant has the potential to combat polymicrobial biofilms related to endodontic infections.

Author Contributions: Conceptualization, O.S.S.; methodology, O.S.S.; software, O.S.S.; validation, H.K.A./L.K., F.D.; formal analysis; investigation, H.K.A./L.K., O.S.S.; resources, F.D. and H.C.; data curation, H.C.; writing—original draft preparation, O.S.S. and K.S.P.; writing—review and editing, O.S.S. and K.S.P.; visualization, O.S.S.; H.K.A./L.K., F.D. and K.S.P.; project administration, F.D.; funding acquisition, O.S.S. Authorship is limited to those who have contributed substantially to the work reported. All authors have read and agreed to the published version of the manuscript.

Funding: This research was funded by the Institutional Review Board of International Medical University, Joint Committee on Research and Ethics under the research project ID- PMHS I-2018 (01).

Institutional Review Board Statement: This study required ethical approval.

Informed Consent Statement: Not applicable.

Data Availability Statement: Not Applicable.

Acknowledgments: The authors thank the labs at the International Medical University (IMU), and MIMOS Research Center for the research experiments and analysis. This work was supported in part by the International Medical University (IMU).

Conflicts of Interest: The authors declare no conflict of interest.

References

1. Tapsell, L.C.; Hemphill, I.; Cobiac, L.; Patch, C.S.; Sullivan, D.R.; Fenech, M.; Roodenrys, S.; Keogh, J.B.; Clifton, P.M.; Williams, P.G.; et al. Health benefits of herbs and spices: The past, the present, the future. *Med. J. Aust.* **2006**, *185*, S1–S24. [[CrossRef](#)] [[PubMed](#)]
2. Triggiani, V.; Resta, F.; Guastamacchia, E.; Sabbà, C.; Licchelli, B.; Ghiyasaldin, S.; Tafaro, E. Role of antioxidants, essential fatty acids, carnitine, vitamins, phytochemicals and trace elements in the treatment of diabetes mellitus and its chronic complications. *Endocr. Metab. Immune Disord. Drug Targets* **2006**, *6*, 77–93. [[CrossRef](#)] [[PubMed](#)]
3. Schmidt, K.; Estes, C.; McLaren, A.; Spangehl, M.J. Chlorhexidine Antiseptic Irrigation Eradicates Staphylococcus epidermidis From Biofilm: An In Vitro Study. *Clin. Orthop. Relat. Res.* **2018**, *476*, 648–653. [[CrossRef](#)] [[PubMed](#)]

4. Sakagami, Y.; Iinuma, M.; Piyasena, K.G.N.P.; Dharmaratne, H.R.W. Antibacterial activity of α -Mangostin against vancomycin-resistant *Enterococci* (VRE) and synergism with antibiotics. *Phytomedicine* **2005**, *12*, 203–208. [[CrossRef](#)]
5. Kaomongkolgit, R.; Jamdee, K.; Chaisomboon, N. Antifungal activity of alpha-mangostin against *Candida albicans*. *J. Oral. Sci.* **2009**, *51*, 401–406. [[CrossRef](#)]
6. Larson, R.T.; Lorch, J.M.; Pridgeon, J.W.; Becnel, J.J.; Clark, G.G.; Lan, Q. The biological activity of alpha-mangostin, a larvicidal botanic mosquito sterol carrier protein-2 inhibitor. *J. Med. Entomol.* **2010**, *47*, 249–257.
7. Fabricius, L.; Dahlén, G.; Öhman, A.E.; Möller, A.J. Predominant indigenous oral bacteria isolated from infected root canals after varied times of closure. *Scand. J. Dent. Res.* **1982**, *90*, 134–144. [[CrossRef](#)]
8. Love, R.M. *Enterococcus faecalis*: A mechanism for its role in endodontic failure. *Int. Endod. J.* **2001**, *34*, 399–405. [[CrossRef](#)]
9. Poptani, B.; Sharaff, M.; Archana, G.; Parekh, V. Detection of *Enterococcus faecalis* and *Candida albicans* in previously root-filled teeth in a population of Gujarat with polymerase chain reaction. *Contemp. Clin. Dent.* **2013**, *4*, 62–66. [[CrossRef](#)]
10. Murad, C.F.; Sassone, L.M.; Faveri, M.; Hirata, R., Jr.; Figueiredo, L.; Feres, M. Microbial diversity in persistent root canal infections investigated by checkerboard DNA-DNA hybridization. *J. Endod.* **2014**, *40*, 899–906. [[CrossRef](#)]
11. Dalhar, H.; Latief, M.; Ketut, S.; Dian, A.W. Effectiveness of flavonoid from mangosteen pericarp (*Garcinia mangostana* L.) as *Enterococcus faecalis* antibiofilm. *Conserv. Dent. J.* **2017**, *7*, 18–22.
12. McComb, D.; Smith, D.C. A preliminary scanning electron microscopic study of root canals after endodontic procedures. *J. Endod.* **1975**, *1*, 238–242. [[CrossRef](#)]
13. Hülsmann, M. Effects of mechanical instrumentation and chemical irrigation on the root canal dentin and surrounding tissues. *Endod. Top.* **2013**, *9*, 55–86. [[CrossRef](#)]
14. Sen, B.H.; Wesselink, P.R.; Türkün, M. The smear layer: A phenomenon in root canal therapy. *Int. Endod. J.* **1995**, *28*, 141–148. [[CrossRef](#)]
15. Di Lenarda, R.; Cadenaro, M.; Sbaizero, O. Effectiveness of 1 mol L⁻¹ citric acid and 15% EDTA irrigation on smear layer removal. *Int. Endod. J.* **2000**, *33*, 46–52. [[CrossRef](#)]
16. Haznedaroglu, F. Efficacy of various concentrations of citric acid at different pH values for smear layer removal. *Oral. Surg. Oral. Med. Oral. Pathol. Oral. Radiol. Endod.* **2003**, *96*, 340–344. [[CrossRef](#)] [[PubMed](#)]
17. Dioguardi, M.; Gioia, G.D.; Illuzzi, G.; Laneve, E.; Cocco, A.; Troiano, G. Endodontic irrigants: Different methods to improve efficacy and related problems. *Eur. J. Dent.* **2018**, *12*, 459–466. [[CrossRef](#)]
18. Mohammadi, Z.; Asgary, S. A comparative study of antifungal activity of endodontic irrigants. *Iran Endod. J.* **2015**, *10*, 144–147. [[PubMed](#)]
19. Mohammadi, Z. Chlorhexidine gluconate, its properties and applications in endodontics. *Iran Endod. J.* **2008**, *2*, 113–125. [[PubMed](#)]
20. Yamashita, J.C.; Tanomaru Filho, M.; Leonardo, M.R.; Rossi, M.A.; Silva, L.A. Scanning electron microscopic study of the cleaning ability of chlorhexidine as a root-canal irrigant. *Int. Endod. J.* **2003**, *36*, 391–394. [[CrossRef](#)]
21. Chang, Y.C.; Huang, F.M.; Tai, K.W.; Chou, M.Y. The effect of NaOCl and CHX on cultured human periodontal ligament cells. *Oral Surg. Oral Med. Oral Pathol. Oral Radiol. Endod.* **2001**, *92*, 446–450. [[CrossRef](#)]
22. Narang, J.K.; Narang, R. Emerging role of nanoemulsions in oral health management. *Int. J. Pharm. Investig.* **2017**, *7*, 1–3. [[CrossRef](#)]
23. Kotta, S.; Khan, A.W.; Pramod, K.; Ansari, S.H.; Sharma, R.K.; Ali, J. Exploring oral nanoemulsions for bioavailability enhancement of poorly water-soluble drugs. *Expert Opin. Drug Deliv.* **2012**, *9*, 585–598. [[CrossRef](#)]
24. Sabjan, K.B.; Munawar, S.M.; Rajendiran, D.; Vinoji, S.K.; Kasinathan, K. Nanoemulsion as Oral Drug Delivery-A Review. *Curr. Drug Res. Rev.* **2020**, *12*, 4–15. [[CrossRef](#)]
25. Liu, Q.; Huang, H.; Chen, H.; Lin, J.; Wang, Q. Food-Grade Nanoemulsions: Preparation, Stability and Application in Encapsulation of Bioactive Compounds. *Molecules* **2019**, *21*, 4242. [[CrossRef](#)]
26. Jhajharia, K.; Parolia, A.; Shetty, K.V.; Mehta, L.K. Biofilm in endodontics: A review. *J. Int. Soc. Prev. Community Dent.* **2015**, *5*, 1–12. [[CrossRef](#)]
27. Hess, D.J.; Henry-Stanley, M.J.; Wells, C.L. The natural surfactant glycerol monolaurate significantly reduces development of *Staphylococcus aureus* and *Enterococcus faecalis* biofilms. *Surg Infect.* **2015**, *16*, 538–542. [[CrossRef](#)]
28. Hinton, A., Jr.; Ingram, K.D. Antimicrobial activity of potassium hydroxide and lauric acid against microorganisms associated with poultry processing. *J. Food Prot.* **2006**, *69*, 1611–1615. [[CrossRef](#)]
29. Devan, K.; Peedikayil, F.C.; Chandru, T.P.; Kottayi, S.; Dhanesh, N.; Suresh, K.R. Antimicrobial efficacy of medium chain fatty acids as root canal irrigants: An in vitro study. *J. Indian Soc. Pedod. Prev. Dent.* **2019**, *37*, 258–264. [[CrossRef](#)]
30. Ghonmode, W.N.; Balsaraf, O.D.; Tambe, V.H.; Saujanya, K.P.; Patil, A.K.; Kakde, D.D. Comparison of the antibacterial efficiency of neem leaf extracts, grape seed extracts and 3% sodium hypochlorite against *E. faecalis*-An in vitro study. *J. Int. Oral Health* **2013**, *5*, 61–66.
31. Gorain, B.; Choudhury, H.; Kundu, A.; Sarkar, L.; Karmakar, S.; Jaisankar, P.; Pal, T.K. Nanoemulsion strategy for olmesartan medoxomil improves oral absorption and extended antihypertensive activity in hypertensive rats. *Colloids Surf. B Biointerfaces* **2014**, *115*, 286–294. [[CrossRef](#)] [[PubMed](#)]
32. Choudhury, H.; Zakaria, N.F.B.; Tilang, P.A.B.; Tzeyung, A.S.; Pandey, M.; Chatterjee, B.; Alhakamy, N.A.; Bhattamishra, S.K.; Kesharwani, P.; Gorain, B.; et al. Formulation development and evaluation of rotigotine mucoadhesive nanoemulsion for intranasal delivery. *J. Drug Deliv. Sci. Technol.* **2019**, *54*, 101301. [[CrossRef](#)]

33. Chong, W.T.; Tan, C.P.; Cheah, Y.K.; Lajis, A.F.B.; Habi Mat Dian, N.L.; Kanagaratnam, S.; Lai, O.M. Optimization of process parameters in preparation of tocotrienol-rich red palm oil-based nanoemulsion stabilized by Tween80-Span 80 using response surface methodology. *PLoS ONE* **2018**, *13*, e0202771. [[CrossRef](#)] [[PubMed](#)]
34. Kumbhar, S.A.; Kokare, C.R.; Shrivastava, B.; Gorain, B.; Choudhury, H. Preparation, characterization, and optimization of asenapine maleate mucoadhesive nanoemulsion using Box-Behnken design: In vitro and in vivo studies for brain targeting. *Int. J. Pharm.* **2020**, *30*, 119499. [[CrossRef](#)]
35. Akrawi, S.H.; Gorain, B.; Nair, A.B.; Choudhury, H.; Pandey, M.; Shah, J.N.; Venugopala, K.N. Development and Optimization of Naringenin-Loaded Chitosan-Coated Nanoemulsion for Topical Therapy in Wound Healing. *Pharmaceutics* **2020**, *20*, 893. [[CrossRef](#)]
36. Hofherr, L.; Votava, H.; Blazevic, D.J. Comparison of three methods for identifying nonfermenting gram-negative rods. *Can. J. Microbiol.* **1978**, *24*, 1140–1144. [[CrossRef](#)]
37. Otto, L.A.; Blachman, U. Nonfermentative bacilli: Evaluation of three systems for identification. *J. Clin. Microbiol.* **1979**, *10*, 147–154. [[CrossRef](#)]
38. Owuama, C.I. Determination of minimum inhibitory concentration (MIC) and minimum bactericidal concentration (MBC) using a novel dilution tube method. *Afr. J. Microbiol. Res.* **2017**, *11*, 977–980.
39. Wu, G.; Yang, Q.; Long, M.; Guo, L.; Li, B.; Meng, Y.; Zhang, A.; Wang, H.; Liu, S.; Zou, L. Evaluation of agar dilution and broth microdilution methods to determine the disinfectant susceptibility. *J. Antibiot.* **2015**, *68*, 661–665. [[CrossRef](#)]
40. Coffey, B.M.; Anderson, G.G. Biofilm formation in the 96-well microtiter plate. In *Pseudomonas Methods and Protocols*; Humana Press: New York, NY, USA, 2014; pp. 631–641.
41. Haapasalo, M.; Ørstavik, D. In vitro infection and disinfection of dentinal tubules. *J. Dent. Res.* **1987**, *66*, 1375–1379. [[CrossRef](#)]
42. Galán, C.; Ariatti, A.; Bonini, M.; Clot, B.; Crouzy, B.; Dahl, A.; FernandezGonzález, D.; Frenguelli, G.; Gehrig, R.; Isard, S.; et al. Recommended terminology for aerobiological studies. *Aerobiologia* **2017**, *33*, 293–295. [[CrossRef](#)]
43. Chum, J.D.; Lim, D.J.Z.; Sheriff, S.O.; Pulikkotil, S.J.; Suresh, A.; Davamani, F. In vitro evaluation of octenidine as an antimicrobial agent against *Staphylococcus epidermidis* in disinfecting the root canal system. *Restor. Dent. Endod.* **2019**, *8*, e8.
44. Andrabi, S.M.; Kumar, A.; Tewari, R.K.; Mishra, S.K.; Iftekhhar, H. An In Vitro SEM Study on the Effectiveness of Smear Layer Removal of Four Different Irrigations. *Iran Endod. J.* **2012**, *7*, 171–176.
45. Hülsmann, M.; Rummelin, C.; Schäfers, F. Root canal cleanliness after preparation with different endodontic handpieces and hand instruments: A comparative SEM investigation. *J. Endod.* **1997**, *23*, 301–306. [[CrossRef](#)]
46. Matt, C.; Jennifer, S.C. *Guide to Research Techniques in Neuroscience*, 2nd ed.; Elsevier Publication: Amsterdam, The Netherlands, 2010.
47. Ngo, Y.X.; Haga, K.; Suzuki, A.; Kato, H.; Yanagisawa, H.; Izumi, K.; Sada, A. Isolation and Culture of Primary Oral Keratinocytes from the Adult Mouse Palate. *J. Vis. Exp.* **2021**, *24*, 175.
48. Saberi, A.H.; Fang, Y.; McClements, D.J. Effect of glycerol on formation, stability, and properties of vitamin-E enriched nanoemulsions produced using spontaneous emulsification. *J. Colloid Interface Sci.* **2013**, *411*, 105–113. [[CrossRef](#)]
49. Posocco, P.; Perazzo, A.; Preziosi, V.; Laurini, E.; Priclab, S.; Guidocde, S.; Posocco, P. Interfacial tension of oil/water emulsions with mixed non-ionic surfactants: Comparison between experiments and molecular simulations. *RSC Adv.* **2016**, *6*, 4723–4729. [[CrossRef](#)]
50. Algahtani, M.S.; Ahmad, M.Z.; Ahmad, J. Investigation of Factors Influencing Formation of Nanoemulsion by Spontaneous Emulsification: Impact on Droplet Size, Polydispersity Index, and Stability. *Bioengineering* **2022**, *9*, 384. [[CrossRef](#)]
51. Sarheed, O.; Dibi, M.; Ramesh, K.V.R.N.S. Studies on the Effect of Oil and Surfactant on the Formation of Alginate-Based O/W Lidocaine Nanocarriers Using Nanoemulsion Template. *Pharmaceutics* **2020**, *17*, 1223. [[CrossRef](#)]
52. Vasconcelos, B.C.de.; Luna-Cruz, S.M.; De-Deus, G.; Moraes, I.G.D.; Maniglia-Ferreira, C.; Gurgel-Filho, E.D. Cleaning ability of chlorhexidine gel and sodium hypochlorite associated or not with EDTA as root canal irrigants: A scanning electron microscopy study. *J. Appl. Oral Sci.* **2007**, *15*, 387–391. [[CrossRef](#)]
53. Karkehabadi, H.; Yousefifakhr, H.; Zadsirjan, S. Cytotoxicity of Endodontic Irrigants on Human Periodontal Ligament Cells. *Iranian Endodontic Journal.* **2018**, *13*, 390–394. [[PubMed](#)]
54. Scelza, M.Z.; de Noronha, F.; da Silva, L.E.; Maurício, M.; Gallito, M.A.; Scelza, P. Effect of Citric Acid and Ethylenediaminetetraacetic Acid on the Surface Morphology of Young and Old Root Dentin. *Iran Endod. J.* **2016**, *11*, 188–191. [[PubMed](#)]
55. Bystrom, A.; Sundqvist, G. The antibacterial action of NaOCl and EDTA in 60 cases of endodontic therapy. *Int. Endod. J.* **1985**, *18*, 35–40. [[CrossRef](#)] [[PubMed](#)]
56. Sedgley, C.; Buck, G.; Appelbe, O. Prevalence of *Enterococcus faecalis* at multiple oral sites in endodontic patients using culture and PCR. *J. Endod.* **2006**, *32*, 104–109. [[CrossRef](#)] [[PubMed](#)]
57. Stuart, C.H.; Schwartz, S.A.; Beeson, T.J.; Owatz, C.B. *Enterococcus faecalis*: Its role in root canal treatment failure and current concepts in retreatment. *J. Endod.* **2006**, *32*, 93–98. [[CrossRef](#)]
58. Waltimo, T.M.T.; Siren, E.K.; Torkko, H.L.; Olsen, I.; Haapasalo, M.P. Fungi in therapy-resistant apical periodontitis. *Int. Endod. J.* **1997**, *30*, 96–101. [[CrossRef](#)]
59. Peciuliene, V.; Reynaud, A.H.; Balciuniene, I.; Haapasalo, M.P.P. Isolation of yeasts and enteric bacteria in root-filled teeth with chronic apical periodontitis. *Int. Endod. J.* **2001**, *34*, 429–434. [[CrossRef](#)]

60. Egan, M.W.; Spart, D.A.; Ng, Y.L.; Lam, J.M.; Moles, D.R.; Gulabivala, K. Prevalence of yeast in saliva and root canals of teeth associated with apical periodontitis. *Int. Endod. J.* **2002**, *35*, 321–329. [[CrossRef](#)]
61. Röhner, E.; Jacob, B.; Böhle, S.; Rohe, S.; Löffler, B.; Matziolis, G.; Zippelius, T. NaOCl is more effective than CHX for eradication of bacterial biofilm of *staphylococci* and *Pseudomonas aeruginosa*. *Knee Surg. Sport. Traumatol. Arthrosc.* **2020**, *28*, 3912–3918. [[CrossRef](#)]
62. Hidajat, M.J.; Jo, W.; Kim, H.; Noh, J. Effective Droplet Size Reduction and Excellent Stability of Limonene Nanoemulsion Formed by High-Pressure Homogenizer. *Colloids Interfaces* **2020**, *4*, 5. [[CrossRef](#)]
63. Đorđević, S.M.; Cekić, N.D.; Savić, M.M.; Isailović, T.M.; Randelović, D.V.; Marković, B.D.; Savić, S.R.; Timić Stamenić, T.; Daniels, R.; Savić, S.D. Parenteral nanoemulsions as promising carriers for brain delivery of risperidone: Design, characterization and in vivo pharmacokinetic evaluation. *Int. J. Pharm.* **2015**, *493*, 40–54. [[CrossRef](#)]
64. Eid, A.; Elmarzugi, N.; El Enshasy, H. Preparation and evaluation of olive oil nanoemulsion using sucrose monoester. *Int. J. Pharm. Pharm. Sci.* **2013**, *5*, 434–440.
65. Danaei, M.; Dehghankhold, M.; Ataei, S.; Hasanzadeh, D.F.; Javanmard, R.; Dokhani, A.; Khorasani, S.; Mozafari, M.R. Impact of Particle Size and Polydispersity Index on the Clinical Applications of Lipidic Nanocarrier Systems. *Pharmaceutics* **2018**, *18*, 57. [[CrossRef](#)]
66. Kaomongkolgit, R.; Jamdee, K.; Pumklin, J.; Pavasant, P. Laboratory evaluation of the antibacterial and cytotoxic effect of alpha-mangostin when used as a root canal irrigant. *Indian J. Dent.* **2013**, *4*, 12–28. [[CrossRef](#)]
67. Sivaranjani, M.; Prakash, M.; Gowrishankar, S.; Rathna, J.; Pandian, S.K.; Ravi, A.V. In vitro activity of alpha-mangostin in killing and eradicating *Staphylococcus epidermidis* RP62A biofilms. *Appl. Microbiol. Biotechnol.* **2017**, *101*, 3349–3359. [[CrossRef](#)]
68. Ibrahim, M.Y.; Hashim, N.M.; Mariod, A.A.; Mohan, S.; Abdulla, M.A.; Abdelwahab, S.I.; Arbab, I.A. α -Mangostin from *Garcinia mangostana* Linn: An updated review of its pharmacological properties. *Arab. J. Chem.* **2016**, *9*, 31–329. [[CrossRef](#)]
69. Leelapornpisid, W. Efficacy of alpha-mangostin for antimicrobial activity against endodontopathogenic microorganisms in a multi-species bacterial-fungal biofilm model. *Arch. Oral Biol.* **2022**, *133*, 105304. [[CrossRef](#)]
70. Nourzadeh, M.; Amini, A.; Fakoor, F.; Raoof, M.; Sharififar, F. Comparative Antimicrobial Efficacy of *Eucalyptus Galbie* and *Myrtus Communis* L. Extracts, Chlorhexidine and Sodium Hypochlorite against *Enterococcus Faecalis*. *Iran Endod. J.* **2017**, *12*, 205–210.
71. Smith, D.C.; Maiman, R.; Schwechter, E.M.; Kim, S.J.; Hirsh, D.M. Optimal irrigation and debridement of infected total joint implants with chlorhexidine gluconate. *J. Arthroplasty.* **2015**, *30*, 1820–1822. [[CrossRef](#)]
72. Vianna, M.E.; Gomes, B.P.; Berber, V.B.; Zaia, A.A.; Ferraz, C.C.; de Souza-Filho, F.J. In vitro evaluation of the antimicrobial activity of chlorhexidine and sodium hypochlorite. *Oral Surg. Oral Med. Oral Pathol. Oral Radiol. Endod.* **2004**, *97*, 79–84. [[CrossRef](#)]
73. Radcliffe, C.E.; Potouridou, L.; Qureshi, R.; Hababbeh, N.; Qualtrough, A.; Worthington, H.; Drucker, D.B. Antimicrobial activity of varying concentrations of sodium hypochlorite on the endodontic microorganisms *Actinomyces israelii*, *A. naeslundii*, *Candida albicans* and *Enterococcus faecalis*. *Int. Endod. J.* **2004**, *37*, 438–446. [[CrossRef](#)] [[PubMed](#)]
74. Sakinah, A.; Setyowati, L. The cleanliness differences of root canal irrigated with 0.002% saponin of mangosteen peel extract and 2.5% NaOCl. *Dent. J.* **2015**, *48*, 104–107. [[CrossRef](#)]
75. Charlie, K.M.; Kuttappa, M.A.; George, L.; Manoj, K.V.; Joseph, B.; John, N.K. A Scanning Electron Microscope Evaluation of Smear Layer Removal and Antimicrobial Action of Mixture of Tetracycline, Acid and Detergent, Sodium Hypochlorite, Ethylenediaminetetraacetic Acid, and Chlorhexidine Gluconate: An In vitro Study. *J. Int. Soc. Prev. Community Dent.* **2018**, *8*, 62–69.
76. Niyonsaba, F.; Ushio, H.; Nakano, N.; Ng, W.; Sayama, K.; Hashimoto, K.; Nagaoka, I.; Okumura, K.; Ogawa, H. Antimicrobial peptides human beta-defensins stimulate epidermal keratinocyte migration, proliferation and production of proinflammatory cytokines and chemokines. *J. Investig. Dermatol.* **2007**, *27*, 594–604. [[CrossRef](#)] [[PubMed](#)]
77. Grone, A. Keratinocytes and cytokines. *Vet. Immunol. Immunopathol.* **2002**, *6*, 1–12. [[CrossRef](#)]
78. Sfakianakis, A.; Barr, C.E.; Kreutzer, D.L. Localization of the chemokine interleukin-8 and interleukin-8 receptors in human gingiva and cultured gingival keratinocytes. *J. Periodontal. Res.* **2002**, *37*, 154–160. [[CrossRef](#)]
79. Abate, M.; Pagano, C.; Masullo, M.; Citro, M.; Pisanti, S.; Piacente, S.; Bifulco, M. Mangostanin, A Xanthone Derived from *Garcinia mangostana* Fruit, Exerts Protective and Reparative Effects on Oxidative Damage in Human Keratinocytes. *Pharmaceutics* **2022**, *15*, 84. [[CrossRef](#)]
80. Ngawhirunpat, T.; Opanasopi, P.; Sukma, M.; Sittisombut, C.; Kat, A.; Adachi, I. Antioxidant, free radical-scavenging activity and cytotoxicity of different solvent extracts and their phenolic constituents from the fruit hull of mangosteen (*Garcinia mangostana*). *Pharm. Biol.* **2010**, *48*, 55–62. [[CrossRef](#)]

Disclaimer/Publisher’s Note: The statements, opinions and data contained in all publications are solely those of the individual author(s) and contributor(s) and not of MDPI and/or the editor(s). MDPI and/or the editor(s) disclaim responsibility for any injury to people or property resulting from any ideas, methods, instructions or products referred to in the content.